Development of an *In Vitro* Assay for High-Throughput Screening Investigating the Role of Mesenchymal Stem Cells on Castration Resistant Prostate Cancer Cell Growth

Alexander Williamson

MSc by Research, Molecular and Clinical Medicine (ECRC)

University of Edinburgh

2017

Principal Supervisor: Dr Bin-Zhi Qian

Co-supervisor: Professor Neil Carragher

Declaration

I, Alexander Williamson, hereby declare that:

a) This dissertation has been composed by me and me alone;
b) The work presented within this dissertation is my own;
c) This dissertation has not been submitted for any other degree or professional qualification except as specified

Signature: ……………………………………………………………… Date:…………………………………………........

Abstract

Androgen deprivation therapy (ADT) can increase survival from prostate cancer by up to 2-3 years, but tumours invariably relapse into an ADT-unresponsive, incurable form, known as castrate resistant prostate cancer (CRPC). CRPC is more aggressive and more likely to metastasise to bone, worsening morbidity and mortality. Mesenchymal stem cells have been implicated in alteration of androgen signalling within prostate cancer cells and stimulation of metastasis and resistance to anti-tumour therapy, and thus may play an important role in the development of castration resistance. A high throughput screen to identify compounds that inhibit the effect of MSCs on castration resistance would thus be valuable in development of novel chemotherapeutics against CRPC.

Clones of the human CWR22PC and murine Myc-CaP Bo prostate cancer cell lines were characterised by their reduced growth in response to androgen deprivation, modelled using charcoal stripped serum and the antiandrogen enzalutamide. Investigations were performed to optimise the miniaturisation of this assay. The effect of conditioned media from human or murine mesenchymal stem cells on this cell growth was then examined in the presence of androgen and androgen deprivation, in a high-throughput format.

It was found that MSC-conditioned media had only a small positive effect stimulating growth in CWR22PC cells, greatest in the enzalutamide-treated condition. In the murine Myc-CaP Bo cell line clone 5GSH-6943#5, MSC-conditioned media significantly stimulated castration-resistant growth in the androgen deprivation condition but not in the presence of androgen. However, assay validation indicated that the assay developed for either cell line was not suitable for high-throughput drug screening in its current form. Further optimisation is thus required for use of the assays developed as a platform for high-throughput screening to investigate the effects of various therapeutic compounds on MSC stimulation of castration-resistant prostate cancer cell growth.

Lay Summary

Prostate cancer is the most common cancer in males and amongst all cancers is the second greatest killer of men. The growth of prostate cancer at first requires the hormone testosterone; most successful treatments against the cancer have relied upon greatly reducing the amount of testosterone in the body by physical or chemical castration, or preventing testosterone that is present from stimulating cancer cells: this is known as androgen deprivation therapy (ADT). These treatments are effective at controlling prostate cancer for up to 2 or 3 years, but eventually stop working. After this happens, the cancer once again grows quickly and aggressively and is more likely to spread to the bones, increasing the risk of both death and complications such as bone fractures and pain, which often significantly harm quality of life.

The reasons for this appear to involve changes in the way cells of the prostate cancer respond to testosterone. These changes may be brought about with the help of other, non-cancerous cells associated with the tumour, in particular a type of bone marrow stem cell known as a mesenchymal stem cell (MSC). This study involves the design of a method of investigating the effect MSCs may have on prostate cancer cells and their sensitivity to testosterone withdrawal.

It was found that secreted factors from MSCs stimulated growth of human and mouse prostate cancer cells, and that this effect was greatest when cells were deprived of testosterone. This experiment may form the basis of a drug screening program to investigate many different chemical compounds for their potential to improve the effects of ADT, and reduce the stimulation of prostate cancer cell growth by MSCs during androgen deprivation therapy. Such a study would be a step forward in improving and lengthening the lives of men with prostate cancer. However, the experimental methods developed in this project need further improvement to be of sufficient quality for use in such drug screening.

Contents

Acknowledgements

I would like to express my most sincere thanks to Dr Bin-Zhi Qian, my principal supervisor, for his guidance, encouragement and direction constantly over the course of the project. His patience and willingness to so readily provide me advice and respond to my queries have been essential to everything I have achieved in this degree. I am also deeply grateful to my assistant supervisor Prof. Neil Carragher, who has always been approachable and willing to offer guidance on drug screening and many other aspects of my project, and for use of facilities such as the IncuCyte Zoom in the Edinburgh Phenotypic Assay Centre (EPAC) lab.

Special thanks must also be given to Dr Galadrielle Biver, for her invaluable help and guidance with almost all aspects of my project, not least for generating and providing me with CWR22PC and primary mesenchymal stem cells, and for her advice and supervision in cell culture. I would also like to give special thanks to Dr Richard Elliott, for his help and guidance in cell culture and expertise in scaling and optimisation of the assay to a 96-well format, and for his constant support and approachability whenever I have been unsure about any aspect of my project.

I would also like to thank Dr Xue-Feng Li, Dr Ashley Dorning, Dr Dahlia Doughty Shenton, Dr Shuiqing Wu, Nicola Graham and Ruoyu Ma: all have different times provided me with crucial advice and support when inexperience had left me unsure of the best course of action, and have all contributed to my training and teaching of research science over the course of my MSc. Thanks also to Dr Steven Pollard for his input and guidance as part of my MSc committee, and to Professor Jeffrey Pollard and all members of the Pollard and Miron labs.

Abbreviations

ADT: Androgen deprivation therapy
ANOVA: Analysis of variance
AR: Androgen receptor
ARE: Androgen response element
BME: Basal Medium Eagle
BM-MSC: Bone marrow mesenchymal stem cell
BMP: Bone morphogenic protein
CAF: Cancer-associated fibroblast
CCL/ CXCL: Chemokine ligand
cDNA: Complementary DNA
CM: Conditioned media
CRPC: Castration resistant prostate cancer
CSC: Cancer stem cell
CSS: Charcoal stripped serum
CV: Coefficient of variance
DHEA: Dehydroepiandrosterone
DHT: Dihydrotestosterone
DMEM: Dulbecco's Modified Eagle's medium
DMSO: Dimethyl sulphide
EC50: Half maximal effective concentration
ECM: Extracellular matrix
EDTA: Ethylenediaminetetraacetic acid
EGFR: Epidermal growth factor receptor
EMT: Epithelial-mesenchymal transition
FBS: Fetal bovine serum
GnRH: Gonadotropin-releasing hormone
HSC: Haematopoietic stem cell
HTS: High throughput screening
IC50: Half maximal inhibitory concentration
IGF: Insulin-like growth factor
IL: Interleukin
iRFP: Infrared fluorescent protein
LBD: Ligand binding domain
LHRH: Luteinising hormone-releasing hormone
mCRPC: Metastatic castration-specific prostate cancer
MDV/ MDV3100: Enzalutamide
MMP: Matrix metalloproteinase
MSC: Mesenchymal stem cell
MTT: 3-(4,5-Dimethylthiazol-2-yl)-2,5-Diphenyltetrazolium Bromide
OD: Optical density
PBS: Phosphate-buffered saline
PCa: Prostate cancer
PCR: Polymerase chain reaction
PGE2: Prostaglandin E2
PS: Penicillin-Streptomycin
PSA: Prostate-specific antigen
PTEN: Phosphatase and tensin homolog
ROS: Reactive oxygen species
SDF1: Stromal cell-derived factor 1
S.E.M: Standard error of mean
shRNA: Short hairpin ribonucleic acid
TGFβ: Transforming growth factor beta
TNFα: Tumour necrosis factor alpha
VEGF: Vascular endothelial growth factor

Chapter 1 | Introduction

1.1.1 | Castration resistant prostate cancer

In men, prostate cancer is the most common type overall and the second most common cause of cancer death, accounting for 28% of new cancer cases and 10% of deaths from cancer in men in the US: over the course of his lifetime a man has a one in six probability of developing invasive prostate cancer [1]. In the UK, there were 46,700 new cases of prostate cancer in 2014, of which roughly 4 in 10 were diagnosed at a late stage, and 11,300 deaths [2]. This disease thus poses a large burden on male quality of life and on health services. When it arises, prostate cancer (PCa) growth is dependent on androgen, and therefore first line treatment for metastatic prostate cancer is androgen deprivation therapy (ADT). Androgen deprivation therapy induces remission of the tumour for 2-3 years [3], however, invariably the tumour develops resistance to ADT and relapses as castration resistant prostate cancer (CRPC). After relapse, tumours are particularly aggressive, with mean survival time only 16-18 months [3]. Medical advances have caused significant improvements in prostate cancer death rates: 10 year-survival in the UK is 84%, compared to around a quarter in the 1970s. A significant amount of this decline in mortality is due to PSA screening allowing earlier detection [2].

Castration resistant prostate cancer is particularly associated with bone metastasis, present in over 90% cases, most commonly in the spine [4]. In addition, highly metastatic prostate cancer is more likely to become castration-resistant [5,6]. There is evidence of a link between a highly invasive prostate cancer phenotype and castration resistance: for example, Shiota et al (2015) found that more highly invasive CWR22Rv1 clones showed higher AR expression and growth rate in the absence of androgen [6]. Bony metastases have a profoundly negative effect on prognosis in terms of both mortality and morbidity, with osteoblastic bone metastases causing complications such as pain, spinal cord compression, pathologic fractures and hypercalcaemia, with a significant negative effect on quality of life. Androgen deprivation therapy itself is also associated with osteoporosis and increased risk of fracture [7], although adjuvant bisphosphonates can be prescribed to reduce this [8,9].

1.1.2 | Androgen deprivation therapy and treatment of prostate cancer

The discovery of androgen deprivation as a treatment for prostate cancer was made by Charles Huggins *et al* in 1941, who found that orchidectomy or administration of oestrogen induced tumour regression in all cases but one, and reduced pain from bony metastases [10]. Orchidectomy was later superseded in many cases by LHRH and GnRH analogues, which provided equivalent increases in survival, but were of course much less invasive [11,12]. These analogues caused an initial sharp increase in testosterone production followed by feedback inhibition of secretion: the negative effects of this 'testosterone flare' led to development of LHRH and GnRH antagonists, which act to inhibit testosterone secretion without the initial flare [13]. Later, agents acting to block the androgen receptor directly were introduced, such as cyproterone. These first-generation antiandrogens were followed by non-steroidal antiandrogens, such as flutamide and bicalutamide, which lacked central and progestational side effects of their forebears, including impotence and reduced libido [11]. However, these drugs have several-fold lower affinity for the AR than androgens and their function is vulnerable to AR mutations in the ligand binding domain (LBD) causing them to act as partial agonists, reducing the effectiveness of AR inhibition [11,14].

The shortcomings of these drugs led to the development of 2nd generation antiandrogens such as enzalutamide (MDV3100, brand name Xtandi). Enzalutamide does not only block testosterone binding to the AR but also inhibits nuclear translocation, recruitment of cofactors and binding to DNA [15]. This would mostly prevent partial agonist effects [16], although AR mutations have been identified which confer agonism of enzalutamide [17]. Enzalutamide has been found to be have substantially higher antitumour activity compared to bicalutamide in mouse xenograft models [15]. In patients, enzalutamide improves survival in metastatic CRPC that does not respond to other forms of ADT: in the AFFIRM phase 3 trial, it was found to decrease risk of death by 37% compared to a placebo in patients with metastatic CRPC previously treated with docetaxel, and outperformed the placebo at all secondary end points [18]. The benefit of enzalutamide in CRPC supports the idea that AR signalling may be still required for growth and maintenance of the tumour, even under castrate levels of testosterone [19].

Only 8% of prostate cancer patients in the UK are treated by major surgical resection of the tumour, with resection more likely in younger patients and not recommended for patients aged above 75 [20]. Prostate cancer tends to be less aggressive in older patients: due to low mortality, therefore, resection of the tumour in these patients often does more harm than good [20]. However, the morbidity of metastasis highlights the importance of treatment. Risk of metastatic progression may be assessed by PSA level: low risk localised disease is generally managed by active surveillance, including periodic PSA testing, digital examination, prostate biopsies and MRI scanning. High risk localised prostate cancer may be treated with radical prostatectomy or radiotherapy; pelvic radiotherapy is also used in locally advanced disease, and may be combined with high-dose rate brachytherapy or androgen deprivation therapy in intermediate and high risk localised disease [9]. When given alone for early stage prostate cancer, ADT does not appear to give any survival benefit and may actually worsen survival [5,21].

Long term ADT, which may be administered intermittently, is used to treat locally advanced and metastatic prostate cancer. LHRH agonists such as goserelin or buserelin are the main form of ADT prescribed in the UK; the antiandrogen cyproterone acetate may also be given prophylactically against testosterone flare [22]. The GnRH antagonist degarelix is recommended for hormone sensitive PCa which has metastasised to bone [23]. Bilateral orchidectomy is also offered to all men, but anti-androgen therapy is not used first-line in metastatic PCa. Castration resistant prostate cancer is treated first line by docetaxel and corticosteroid therapy [22], with antiandrogens often administered after the failure of first line treatments [7]: in the UK, enzalutamide is given to men with prostate cancer refractory to docetaxel and other forms of ADT [24]. Notably, enzalutamide and bicalutamide have been reported to stimulate invasion of prostate cancer cells by promoting macrophage migration to them, to enhance CCL2 signalling and to increase the number of distant metastases in the diaphragm and lymph nodes [25].

1.1.3 | Dysregulation of androgen receptor signalling is associated with progression to CRPC

The androgen receptor (AR) is an intracellular steroid hormone receptor activated by the ligands testosterone and dihydrotestosterone (DHT). In the prostate, testosterone, produced mainly in the testes, is reduced to DHT, which is a more potent agonist of the AR, with an EC_{50} of 0.13 compared to 0.66 for testosterone [26,27]. The AR consists of three functional domains: the N-terminal regulatory domain, the ligand-binding domain (LBD), and the DNA binding domain. Upon androgen binding, the receptor-ligand complex undergoes a conformational change, dissociates from heat-shock proteins, and translocates to the nucleus, where it dimerises and with an array of coactivator and corepressor molecules modulates expression of many androgen-responsive genes, for example PSA, by action on androgen-response elements (AREs) [11,27].

The fact that AR expression usually persists even in castrate resistant cancer [28], and that enzalutamide continues to have efficacy in metastatic CRPC resistant to other antiandrogens [18], strongly suggests that CRPC growth remains dependent on AR signalling, even when testosterone is reduced to castrate levels. Multiple mechanisms involving androgen signalling have been proposed to explain progression to CRPC: some of these are summarised in Figure 1. Firstly, mutations in the AR ligand binding domain can allow for stimulation by non-androgenic ligands [16]. For example, the T877A point mutation in AR, when selectively mutated in mouse prostate epithelium, caused prostate hypertrophy and growth stimulation by oestrogen and the AR antagonist bicalutamide. Whilst this mutation did not induce prostate cancer formation alone, it accelerated tumorigenesis in the TRAMP mouse model of prostate cancer, and after castration there was less reduction in tumour growth in mutated compared to control mice [29]. In addition, cells of the androgen-sensitive cell line CWR22PC and the castration resistant CWR22Rv1 line both express the H874Y mutation in the AR LBD, as do CWR22 tumours from which these cell lines are derived. This mutation has been shown to increase the agonist response of the AR to DHEA, estradiol, progesterone and hydroxyflutamide several-fold [30]. Castration-sensitive CWR22PC cells possess this mutation, but lack an exon 3 duplication present in CWR22Rv1 cells and relapsed, androgen-insensitive CWR22 tumours [31]: AR with this duplication has been shown to exhibit constitutive nuclear localisation and DNA binding [32]. Whilst enzalutamide was developed partially to avoid the agonist effects of other antiandrogens, other mutations in the AR have been shown to rescue the growth inhibition caused by enzalutamide and cause the drug to act as an agonist at the AR [17]. Notably, AR pathway mutations are present in 71.3% of metastatic CRPC cases, and are exclusive to CRPC over primary prostate cancer [33].

Secondly, downstream AR signalling pathways may be activated by alternative mechanisms without ligand binding to the AR. Significant crosstalk exists between the AR and growth factor signalling pathways [34]: alternative signalling events, (for example, PTEN loss) may bypass the need for androgen signalling entirely [16,27,35]. Receptor tyrosine kinases (including EGFR, IGF-1R and IL-6R), may also activate AR without androgen binding: in particular, the

HER2 receptor, acting through downstream kinases such as Ack2, increases AR activity and becomes overexpressed as prostate cancer progresses to CRPC [36].

Notably, Chen *et al*. (2004) found that PCa tumours expressed higher levels of AR after passage through castrated mice to induce castration resistance; and that introduction of additional AR cDNA to cells conferred a greater growth rate in charcoal stripped serum (CSS) and more tumour formation in castrated animals. Castration resistant growth still required ligand binding, but AR upregulation allowed functional androgen signalling at castrate testosterone concentrations. It appears this change may involve both AR overexpression and changes to levels of cofactor molecules at AR-responsive genes [16]. These findings are supported by other studies reporting average 6-fold higher AR expression in CRPC samples compared to benign hyperplasias [37]. In addition, around 30% of hormone refractory tumours possess gene amplification of the AR, which is not present in androgen dependent PCa, although AR was still significantly upregulated in refractory tumours lacking the amplification: there are thus multiple methods of AR overexpression [37,38]. Notably, mutations in codon 877 were not seen in tumours with AR amplification [38], demonstrating that multiple discrete possible genetic alterations to the AR can give rise to CRPC.

However, these findings appear to be partially contradicted by RNA microarray data from radical prostatectomy samples, showing that whilst elevated AR expression was associated with higher growth rate and reduced survival time before tumour recurrence, AR expression was in fact lower in castration-resistant metastases [39,40]. The authors of this study suggest that AR signalling may still be enhanced in metastases by mutation in AR allowing activation by noncanonical ligands (as previously described [16,41]), or that immunochemistry may not be able to detect increased amounts of mutated AR [39]. It was also found that AR levels tended to be higher in bone metastases, and that increased AR expression was associated with reduced recurrence-free survival [39]. In addition, expression of the stem cell-associated protein nestin has been shown by Kleeberger *et al*. (2007) to be required for metastasis of AT6.3 prostate cancer xenografts, and appears to be dependent on castration resistance. This study found that nestin expression was detectable only in lethal castration-resistant disease and androgen independent PCa cell lines, and undetectable in ADT-naïve tumours, even in metastases [42]. It thus appears that the role of androgen signalling in acquisition of castration resistance is not limited to a single mechanism.

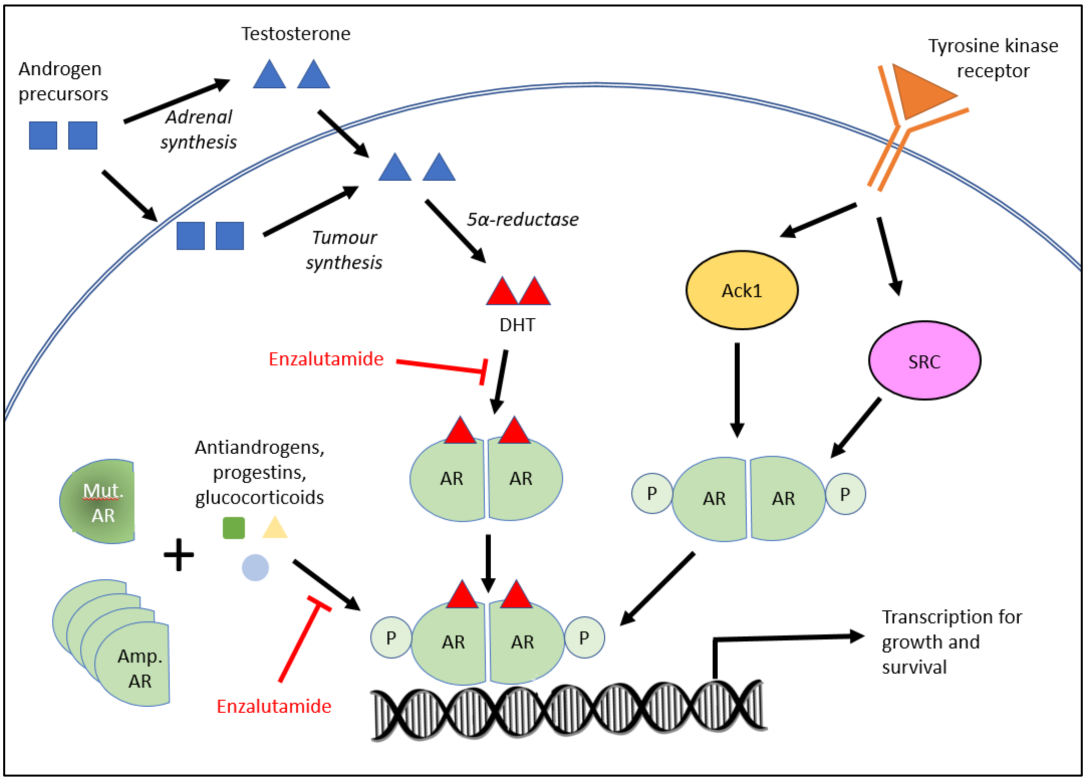

Figure 1: AR signalling and mechanisms of castration resistant AR signalling. The intracellular AR is activated by testosterone or DHT binding, whereupon it translocates to the nucleus and modulates transcription at androgen response elements (AREs). Antiandrogens block this, however AR transcriptional activity may also be activated by tyrosine kinases ("non-genomic" activation) or by overamplified or mutant AR. Adapted from Chen et al (2008) [36].

1.1.4 | AR signalling and ADT have different effects on different cell types in prostate cancer

The effects of androgen signalling in prostate cancer are not limited to tumour cells alone, however. Niu et al (2008) have described how AR signalling in stromal cells promotes PCa progression and invasion, whilst in prostate epithelial cells acts to suppress invasiveness [40]. Effects of androgen also vary between different prostate cell types: prostate epithelial AR signalling was found to suppress proliferation of basal prostate cells (which are mostly AR negative) and promote survival of AR^+ luminal cells [40]. In normal homeostasis, AR signalling is required for differentiation of basal cells into luminal cells and maintenance of luminal cell morphology [43]. Epithelial AR knockout in a murine prostate cancer model leads to expansion of the more highly tumourigenic and metastatic basal and intermediate cells, leading to less differentiated, larger tumours [44]. This is consistent with data showing that ADT and antiandrogens may stimulate prostate cancer progression and metastasis [25]. Contradicting this study, Xie et al (2017) found that although AR knockout in luminal cells caused a burst of proliferation and with cells gaining a more intermediate phenotype, this burst was transient and the cells did not form tumours [43].

When stromal and epithelial AR were knocked out simultaneously at 16 weeks, however, smaller, less differentiated tumours with a lower proliferation and greater apoptosis rate developed: metastasis was suppressed and survival time increased [44]. The effects of ADT on prostate cancer therefore appear to depend on the balance of androgen signalling between different cell types. In the early stages of tumour growth, protumourigenic stromal AR signalling predominates, thus ADT effectively inhibits tumour growth. However, at later stages, alterations to AR signalling and the tumour stroma may cause the expansion of basal and intermediate cells to become the dominant effect, stimulating tumour growth and metastasis [44]. In support of this, a model of enzalutamide-resistant CRPC with combined TP53 and RB1 knockdown showed an increase in basal and neuroendocrine and a decrease in luminal cell markers [45].

1.1.5 | Cells of the tumour stroma form a microenvironmental niche to support tumorigenesis

The role of stromal AR signalling discussed above is only one facet of the vital role played by stromal cells in tumour progression. For example, cancer associated fibroblasts (CAFs) are descendent cells of MSCs which modify the extracellular matrix by production of matrix metalloproteinases (MMPs) to facilitate invasion and metastasis, and recruit a variety of other cell types such as leukocytes and endothelial cells to the tumour environment [46]. These recruited cells may themselves aid tumour progression: for example, M2 macrophages promote tumour growth [47] produce ROS which may cause tumorigenic mutations [48]. Pericytes transitioning into cancer associated fibroblasts have also been implicated in facilitation of invasion and metastasis in fibrosarcomas [49], whilst CAFs in primary breast cancer tumours secrete cytokines which prime cancer cells to metastasise to bone [50].

Signalling crosstalk between stromal cells and with cancer cells forms a tumour niche, comprising beneficial paracrine signalling and microenvironmental conditions to facilitate tumour growth and progression. This is particularly important to facilitate the establishment of new metastases. Stromal cells can form pre-metastatic niches to support cancer cell engraftment before tumour cell arrival or around single disseminated mammary tumour cells [51,52]. In the bone marrow, MSCs and many other stromal cell types maintain the haematopoietic stem cell (HSC) population, but PCa cells usurp this HSC niche to support metastatic growth, forming the bone metastatic niche [53]. Stimulating HSC mobilisation also causes egress of cancer cells, implying the HSC and metastatic niches are maintained by similar mechanisms [54]. Also, breast cancer cells home preferentially to osteoblast-rich areas of bone marrow, suggesting osteoblasts play an important role [55]. This niche also maintains PCa in a dormant cancer stem cell (CSC) phenotype [56], which may confer greater resistance to anticancer therapies [57].

1.1.6 | MSCs home to tumours and stimulate tumour growth

Notably, osteoblasts and fibroblasts are both cells derived from mesenchymal stem cells (MSCs) [58]. MSCs are multipotent cells present mainly in the bone marrow and adipose tissue, with a wide variety of functions including immunosuppression and tissue repair, and have been shown to promote tumour growth and help confer resistance the chemotherapy [58,59]. Under normal circumstances, MSCs are present in the prostate at a low level [60], but are recruited to sites of tumorigenesis due to chronic inflammation and have a number of effects at the primary site, as summarised in Figure 2. The exact mechanisms behind this recruitment are not completely understood, particularly as MSCs are a heterogenous population capable of expressing a wide range of cell trafficking surface molecules, but due in part to their homing to damaged and inflamed tissues, MSCs are believed to be attracted by similar mechanisms to leukocyte recruitment, via chemokines such as CCL5, CXCL2, CCL3, CCL2 and CXCL8 [61]. Expression of these molecules is stimulated by proinflammatory molecules such as VEGF and TNFα secreted by the primary tumour: this secretion may be stimulated through pathways such as HIF-1α produced in response to hypoxic conditions in the tumour [61]. CXCR4-SDF1 interaction has been implicated in MSC trafficking [62,63] to tumour sites, however, other studies have shown blocking CXCR4 did not affect MSC migration to damaged myocardium *in vivo* [64].

Once at the tumour site, MSCs are protumourigenic: for example, co-inoculation of MSCs with PC3 prostate cancer cells was shown to increase tumour proliferation, migration and invasion through a TGFβ-dependent mechanism [65]. IL-6 secretion by MSCs has also been shown to promote tumour cell survival, bone turnover and resistance to cytotoxic therapies [66,67]. MSCs also recruit and interact with immune cells in the niche, with broadly immunosuppressive effects which may help the tumour escape of the immune response [66]; in addition, CXCR2-mediated recruitment of neutrophils by MSCs helps stimulate metastasis in breast cancer [68], whilst recruitment and of macrophages through CCR2 signalling promotes tumour growth [47]. Crosstalk between MSCs and tumour cells is important for development of the tumour microenvironment [53]: TGFβ secreted in exosomes by prostate cancer cells has been shown to stimulate differentiation of MSCs towards a myofibroblastic phenotype, with higher ability to stimulate tumour growth, invasion, and angiogenesis [69].

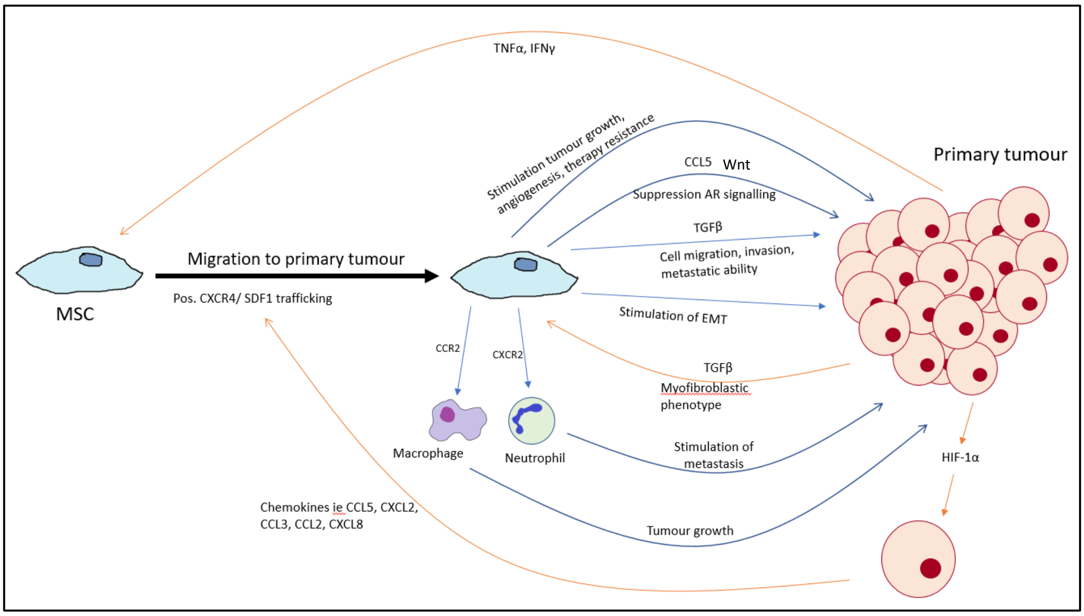

Figure 2: MSCs migrate to the primary tumour due to tumour cell chemokine production and chronic inflammatory signalling. As part of the tumour stroma MSCs stimulate tumour growth, metastasis and other hallmarks of cancer by multiple mechanisms, including TGFβ signalling. MSCs are stimulated by reciprocal signalling from tumour cells. (Spaeth et al (2008) [61], Ridge et al (2017) [71]).

1.1.7 | MSCs stimulate prostate cancer bone metastasis and form part of the bone metastatic niche

MSCs are commonly found in bone marrow [58] and are recruited to the bone marrow niche to aid cancer cell metastasis and growth, through mechanisms summarised in Figure 3. VEGF secreted by the primary tumour in a breast cancer model has been shown to stimulate stromal cell production of prostaglandin E2, which attracts BM-MSCs to aid in formation of a premetastatic niche [53,70]. MSC migration to the niche has also been shown to be stimulated by SDF1 – CXCR4 signalling [62]. In breast cancer, bone marrow MSCs of the niche then attract disseminated cancer cells and facilitate their migration across bone marrow endothelium through secretion of SDF1α [63,71]. Once in the niche, tumour cells modulate MSC and other stromal cell phenotypes to support metastatic growth [53]. IL-6 secretion by MSCs stimulates proliferation and survival of tumour cells, modulation of other stromal cells of the bone marrow niche, and a cancer stem cell phenotype associated with therapy resistance [53,57]. Exosomes from MSCs have been found to induce dormancy and docetaxel resistance in metastatic breast cancer cells in the bone marrow [72], and to induce resistance to multiple chemotherapeutic drugs *in vitro* by secretion of platinum-based fatty acids [59]. This conferred chemoresistance may help PCa cells overcome inhibition by antiandrogens, HSCs of the bone marrow niche stimulate osteoblastic differentiation of MSCs into osteoblasts [71], which have protumourigenic effects and an important role in the bone marrow metastatic niche [53,55].

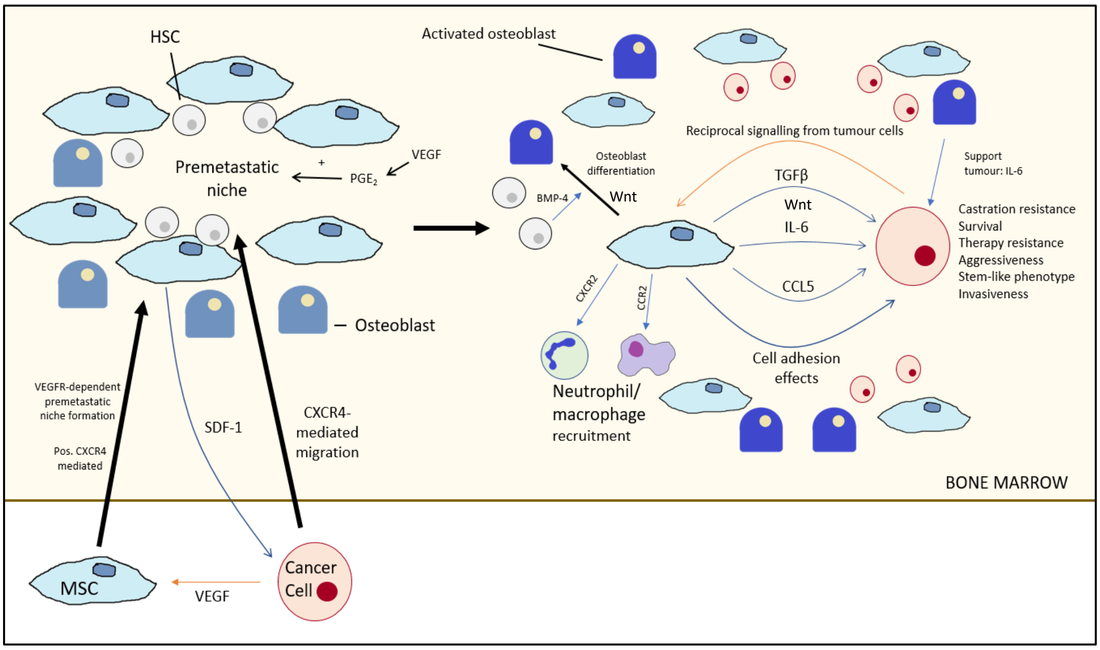

Figure 3: Actions of MSCs at the bone metastatic site. MSCs under normal conditions form part of a HSC niche that may be co-opted by tumour cells, susceptibility to tumour cell engraftment may be increased by prostaglandin E2 as the tumour cells form a premetastatic niche to which tumour cells migrate through SDF-1–CXCR4 signalling. Crosstalk with tumour cells alters the phenotype of MSCs and other stromal cells of the niche to aid tumour growth; MSCs perform many functions to stimulate progression of secondary tumours. (Reagan & Rosen (2015) [53], Corcoran et al. (2008) [63]).

1.1.8 | MSCs contribute to prostate cancer castration resistance

Prostate cancer metastatic ability and castration resistance are closely linked, and influenced by the tumour microenvironment both at the primary site and in the bone metastatic niche. LNCaP prostate cancer cells cultured with prostate or bone stromal cells showed both enhanced castration resistant growth and greater metastatic potential, particularly to lymph nodes and bone, when transplanted into castrated mice [73]. Bone marrow MSCs have also been found to stimulate invasive and metastatic potential and self-renewal ability of prostate cancer cells through a mechanism dependent on suppression of androgen signalling by CCL5: notably, this effect did not occur in PC3 cells where AR is absent [74]. If suppressing androgen signalling stimulates prostate cancer growth and metastasis, as is consistent with other studies that have previously been discussed [25,40,44], this may be a reason why androgen deprivation eventually fails.

In addition to stimulating prostate cancer cell growth and metastasis [65], mesenchymal stem cell TGFβ signalling has also been shown by Cheng et al (2016) to promote castration resistance of LNCaP cells *in vivo* and *in vitro*. In this study, MSC co-injection with LNCaP PCa cells into castrated nude mice increased the castration-resistant growth of resultant tumours. In addition, treatment with MSC-conditioned media almost completely rescued the growth and apoptosis rate of LNCaP cells under androgen deprivation *in vitro*. LNCaPs pre-treated with MSC conditioned media also grew faster than control tumours in castrated mice, to roughly the same tumour volume in non-castrated mice. There was also no additional effect of MSC conditioned media when androgen was present *in vivo* or *in vitro*. These results indicate that, at least in LNCaP cells, the effect of MSCs on tumour growth is predominantly in stimulating castration resistance, and this effect is due mostly to secreted factors. The increase in castration-resistant growth was ablated by shRNA-mediated knockdown of TGFβ in MSCs. Furthermore, it was found that exposure of MSCs to androgen inhibited their expression of TGFβ and greatly reduced their stimulation of castrate resistant growth *in vivo* and *in vitro* [75]. In this case, therefore, androgen deprivation therapy could cause upregulation of MSC TGFβ secretion and thus stimulation of castration-resistant tumour growth, leading to failure of ADT and progression to CRPC. Ye *et. al.* (2012) also found that conditioned media from MSCs contained substantial TGFβ, and administration of TGFβ-blocking antibody inhibited their stimulation of PC3 migration and invasion *in vitro* [65]. MSC TGFβ secretion thus appears to be a link between prostate cancer cell metastatic ability and castration resistance.

Androgen deprivation has also been shown to upregulate both TGFβ1 and TGFβ receptors in prostate cancer cells themselves [76]. Notably, TGFβ may induce epithelial-mesenchymal transition of prostate cancer cells (stimulating metastasis) and stimulate overexpression of the androgen receptor [6], which is associated with castration resistance [16]. Once again this suggests a link between metastasis and CRPC. Other studies suggest downregulation of AR signalling stimulates prostate cancer invasion and growth of the cancer stem cell population [74] – whilst an apparent contradiction, as the authors state, AR may act to suppress metastasis but promote growth and castration resistance [74], and the overall effects of AR signalling may depend upon the stage of tumour progression [44]. The relationship between metastatic ability and therapy resistance has also been demonstrated in other cancers: Yano et al showed that a much higher proportion of invading than non-invading stomach adenocarcinoma cells were in G0/G1 phase, which was associated with increased resistance to cytotoxic therapy [77]. However, human MSCs have been shown to increase the proportion of actively dividing PC-3 prostate cancer cells whilst still stimulating cell division [65].

TGFβ may also act to increase the size of the CSC population and confer resistance to paclitaxel in breast cancer [78]. However, in contradiction of these reports suggesting a role of TGFβ signalling in progression to CRPC, Placencio et al have shown that TGFBR2 knockout in stromal cells induces castration resistance, and that TGFβ acts to maintain androgen sensitivity and enable prostate regression by suppression of Wnt signalling [79]. Notably, castration resistant CWR22Rv1 prostate cancer cells express abnormally low levels of the TGFβ type II receptor [80], and androgen deprivation has been shown to reduce prostate cancer cell TGFBR2 expression [76]. TGFβ1 overproduction and TGFBR2 loss are also associated with poor clinical outcome, however [81]. The effects of TGFβ on androgen sensitivity are thus complex may thus depend on the balance of receptor expression on prostate cancer cells.

In a follow-up study, Placencio et. al. found that bone marrow derived MSCs are recruited to and incorporate into the prostatic epithelia in response to androgen deprivation, likely through the CCL5-CCR5 axis, and stimulate castration resistant growth through paracrine Wnt signalling [82]. Wnt proteins have also been found to be secreted by metastatic prostate cancer cells in the bone marrow, stimulating MSC differentiation into osteoblasts and stimulating formation of osteoblastic bone lesions [83]. Aberrations in Wnt signalling have been found to be present in 18% of mCRPC cases [33], suggesting a role for these pathways in progression to castration resistance.

1.2.1 | Aims and objectives

MSCs are thus implicated through multiple mechanisms in PCa acquisition of castration resistance, both at the primary tumour and the metastatic site. This, and the association between castration resistance and aggressive, bone-metastatic cancers speak to the importance the role MSCs may play in prostate cancer morbidity: inhibiting their effects has potential to greatly improve the lives of prostate cancer patients. The aim of this project was thus to develop a high-throughput assay showing the effects of MSC stimulation on prostate cancer cells both with and without androgen deprivation. This assay could then form the basis of a high throughput screen (HTS) to identify compounds from a drug library which inhibit these effects. Identification of said compounds would help elucidate mechanisms by which MSCs affect prostate cancer response to ADT, and could be further investigated and developed to identify lead compounds for development of new drugs to prolong survival and reduce morbidity from CRPC.

1.2.2 | The present study

The CWR22PC cell line was used as a model of androgen-responsive human prostate cancer. This cell line is derived from highly androgen-sensitive CWR22 prostate tumours, which go into remission upon androgen deprivation for 7-9 months followed by relapse as castration resistant tumours [31,84]. CWR22 xenograft tumours in mice have a much greater response to castration than LNCaP or PC-346 tumours, regressing to a much greater degree and for a longer period before relapse [85]. In addition, CWR22PC cell growth is more reliant on androgen than LNCaP cells both *in vitro* and *in vivo* [31]. CWR22PC cells also possess the H874Y mutation which allows non-androgenic ligands to stimulate the AR [30], a possible mechanism by which progression to CRPC may occur in this cell line. These cells therefore provide a representative model of prostate cancer cells in human tumours before progression to CRPC.

This study also investigated these phenomena in the Myc-CaP murine prostate cancer cell line, isolated from a c-Myc driven transgenic mouse prostate cancer model [86]. These cells have greatly amplified AR but remain androgen-dependent both *in vitro* and *in vivo*, and following androgen deprivation *in vivo* Myc-CaP tumours progress to CRPC. AR amplification is seen 30% of CRPC cases [37,38] and thus this cell line appears to be representative of progression of cells towards castration resistance. In these cells androgen signalling stimulates growth by maintaining expression of the oncogene c-Myc: in Myc-CaP sublines that had become castrate-resistant, c-Myc expression under androgen deprivation was equal or raised compared to androgen-dependent clones, suggesting upregulation of androgen signalling despite castrate levels of androgen [86]. The ability of these cells to transition from hormone-sensitive to refractory suggests they are a good model for investigation of progression to CRPC. These experiments used 5GSH-6943#5 cells, a mixed clone derived from Myc-CaP cells passaged through mice to select cells for cells with propensity to metastasise to bone (unpublished data).

To investigate the response of 5GSH-6943#5 cells to MSC conditioned media, the C3H10T1/2 murine MSC line was used. C3H10T1/2 cells were established from C3H mouse embryos [87], and have been shown to have similar immunosuppressive properties and express similar receptors for immune cell recruitment as primary murine MSCs [88,89], and to promote tumour growth *in vivo* [88]. C3H10T1/2 cells appear to be a good model of bone marrow-derived MSCs, with similar osteogenic and chondrogenic ability, although they are less able to undergo adipogenesis than mouse primary BM-MSCs [90]. As prostate cancer forms osteoblastic lesions, it appears that a cell line with similar osteogenic potential would be a good model. However, whilst *in vivo* and primary BM-MSCs are heterogenous, with different phenotypes and differentiation potentials, the C3H10T1/2 cell line is homogenous [90], and thus fully recapitulate MSC functioning in *in vivo* pathophysiology.

These cells were used in cell viability assays, seeding cells into 24- or 96- well plates and treating with charcoal stripped serum (CSS), enzalutamide (MDV3100), dihydrotestosterone (DHT) and MSC- conditioned media. Charcoal-stripping serum removes non-polar molecules, including androgens, and therefore acts as androgen deprivation. Cell growth over the assay period was measured either by confluence through analysis of microscope images, or by the cell viability assays MTT and CellTiter-Blue. MTT (3-(4,5-Dimethylthiazol-2-yl)-2,5-Diphenyltetrazolium Bromide) is a yellow tetrazolium salt which is reduced by viable cells to formazan, an insoluble dark blue product which can be quantified by absorbance [91]. This reaction occurs intracellularly, catalysed by dehydrogenases on mitochondrial cytochromes B and C [92]. CellTiter-Blue is an assay that functions in a similar manner, in this case by reduction of the blue, nonfluorescent due resazurin to the pink, fluorescent product resorufin. Unlike MTT, which kills the cells, CellTiter-Blue is relatively non-toxic; furthermore, resorufin is excreted into the media from the cells, and thus can be read by fluorescence directly from the plate without further processing [93]. Whilst it is commonly assumed that the reading obtained is directly proportional to cell number, in both assays more metabolically active cells will produce a greater signal.

Initial assays were performed at low throughput in 24 well plates to a previously established lab protocol, and were then miniaturised onto 96 well plates to form the basis of a high-throughput screen. The process of miniaturisation required optimisation to the higher throughput platform, as in order able to identify such compounds, a high assay quality is required, as indicated by a measure such as Z-factor [94]. For optimisation of the time course and starting cell density of the assay, an IncuCyte Zoom live cell imaging system was used to capture kinetic data of cellular confluence by periodic imaging over multiple days. Once the assay was optimised and used to demonstrate the response of the cells to ADT and MSCs, assay validation via min-max signal variability assays was performed to establish suitability for high throughput screening [95].

1.2.3 | High throughput screening

High throughput screening (HTS) compares the effects of many thousands of drugs or other chemicals from a compound library against assay controls. 'Hit' compounds with a detectable positive effect can then be further analysed by dose response and process validation [96]. Such a screen would aim to identify compounds which could increase susceptibility of cells to androgen deprivation and inhibit the protective effect of MSCs. HTS has become one of the primary methods of drug discovery by the pharmaceutical industry [97], and is used both to identify novel lead compounds without identification of a target molecule (a primary screen), or to test and validate compounds identified by other more targeted strategies such as high throughput biological assays (detecting, for example, the concentration of a molecule produced), or investigations based on the structure of receptors or other target molecules. When used as primary screens, analysis of hit compounds may also reveal information about the mechanisms involved in the phenomenon in question. This information may aid in a more targeted approach to drug discovery, investigating compounds affecting these mechanisms: this may involve further high throughput screening using a more targeted drug library. HTS provides the ability to perform many assays in a short time period, allowing testing of many combinations of compounds to detect synergistic effects: for example, screening using the assay designed in this study in human cells would test the effects of both the candidate compound and enzalutamide applied to the cells simultaneously [96].

HTS is frequently used in complementary fashion with other methods of drug discovery: in this way, HTS raises efficiency by allowing very high numbers of experiments to be conducted. Furthermore, automation and biological assay formats used allow for higher levels of precision and sensitivity, and more systemic and unbiased studies. Technology developed for HTS has also led to benefits in other areas of drug discovery, such as lead optimisation [96], whilst processes and techniques have been adapted and expanded to further investigate candidate cancer drugs. High content phenotypic screening may be used to identify compounds causing particular phenotypic changes: for example, candidate angiogenesis inhibitors may be identified by quantifying their effects on endothelial cell tubules using automated imaging systems and specialised analysis algorithms [98]. Such screens can detect changes in multiple modalities simultaneously, and through multiparametric analysis aggregate data to gain detailed information into cellular phenotypic responses. Analysis of this data can then elucidate differences in responses between different cell lines for the same drug or between different drugs. This can provide valuable information regarding drug mechanism of action: for example, by identifying compounds with a similar phenotypic response to a drug with a well understood mechanism [99].

However, the success of HTS in the development of new drugs depends on the physiological relevance of the assay: if it does not represent the true disease situation *in vivo*, then lead compounds identified by HTS are unlikely to have efficacy in the patient. In addition, due to the high number of compounds tested, signal-to-noise ratio must be very low and reproducibility very high to successfully identify hits and avoid false positives. Thirdly, success requires use of an appropriate drug library: particularly in the early years of HTS, libraries were often of limited diversity and contained many compounds, such as dyes, which were very unlikely to produce any effect[96]. HTS is costly, and thus a balance is required between sufficient throughput and size of library, and acceptable cost.

In this project, the androgen sensitivity of prostate cancer cells was characterised using an existing low-throughput protocol. This assay was then adapted onto a higher-throughput format, and various investigations were conducted to optimise the new protocol. The effect of mesenchymal stem cell conditioned media on cell growth and the interaction of this with ADT was then investigated using the high throughput assay. Validation experiments for both human and murine cell assays were then performed to establish the suitability of the assay as a high throughput screening platform: a successful assay would become a starting point for a drug screen to investigate compounds that may inhibit MSC stimulation of castration-resistant prostate cancer cell growth.

Chapter 2 | Materials and Methods

2.1 | Cell culture

All cell lines were cultured in 75 cm^2 flasks, changing media every 3 or 4 days. Cells were passaged when approaching full confluence using 0.05% trypsin-EDTA (Gibco), with the cell suspension centrifuged at 200 x *g* for five minutes and the resulting pellet resuspended in new media before reseeding in a new flask.

CWR22PC cells were cultured in Dulbecco's Modified Eagle Medium (DMEM) (+ 4.5 g/L D-glucose, 2 mM L-glutamine and 1 mM sodium pyruvate) with 10% heat inactivated fetal bovine serum (FBS), 1% Penicillin-Streptomycin (PS) (all purchased from Gibco) and 0.1 nM dihydrotestosterone (DHT) (Sigma-Aldrich). Media was changed completely every 3-4 days. Individual CWR22PC clones used were supplied by Galadrielle Biver after isolation by limiting dilution assay. Prophylactic Plasmocin™ at 5 µg/ml was used to protect clones before cryopreservation.

5GHS-6943#5 were cultured in DMEM + 10% FBS + 1% PS + 1 mg/mL G418 (Geneticin, ThermoFisher). G418 was included to maintain selection for $iRFP^+$ cells. iRFP expression was tested using a CSU-W1 spinning disk confocal microscope (Nikon).

C3H10T1/2 cells were cultured in Basal Medium Eagle (BME) (Gibco) + 10% FBS + 1 mM sodium pyruvate + 2 mM L-glutamine + 1% PS. Cells were used between the 5^{th} and 15^{th} passages only, as per ATCC guidelines.

Primary human MSCs were cultured in DMEM + 10% FBS + 1% PS, changing media every 3-4 days. Effort was made to ensure the pH of the media was not too high and that cells were not removed from the incubator any longer than necessary.

2.2 | Mycoplasma testing

Cells were cultured in antibiotic free media for at least 48 hours to a level near full confluence before removal of media (1mL) from the flask. This media was then taken and centrifuged three times at 13500 x *g* for five minutes each, resuspending in 1 mL PBS each time, before obtaining DNA from the medium via digestion using the Quick Ear Clip method. DNA was then amplified by PCR in a reaction mixture containing 1.25 mM Myc detection primers, (as described by Uphoff and Drexler (2004) [100]), 2X Biomix Red (Bioline), and nuclease-free water (Ambion) in an Applied Biosciences 96 well Thermal Cycler. PCR product was then run on a 2% agarose gel, with a band at 510 base pairs indicating a positive sample.

For testing the new stock 5GSH-6943#5 cells, growth media was collected from cells as before and centrifuged at 200 x *g* for 5 minutes to remove cells. The supernatant was then tested for mycoplasma with the MycoAlert™ Mycoplasma detection kit (Lonza) by Dr Forbes Howie.

5GSH-6943#5 and C3H10T1/2 cells tested positive for mycoplasma and were treated for two to three weeks with Plasmocin™ (InvivoGen) at 25 µg/ml, administered each time cells were passaged (approximately every 3 days)

2.3 | Viability assays

Total viability of cells in each well was measured by either MTT (Sigma-Aldrich) or CellTiter-Blue (Promega) assays after either three or five days. For the MTT assay, 5 mg/mL stock MTT in PBS was added to a final concentration of 250 µg/mL. In 24-well plate experiments, this was achieved by direct addition of the stock MTT solution to the growth media (40 µL into 800 µL media), whilst in 96-well experiments, MTT solution was first diluted 1:20 into DMEM + 10% FBS + 1% PS, before aspiration of media from the wells and replacement with 100 µL solution containing MTT. Plates were then incubated for 1 hour at 37^{o}C 5% CO_2 in darkness, before removal of media and washing with PBS. DMSO was added and the plate shaken to dissolve formazan crystals; absorbance was then read from the samples in a 96-well plate at 540 nm using a LabSystems Multiskan EX microplate reader. Three wells containing the same volume of DMSO only were read to give a background reading which was then subtracted from the OD values for each well.

For the CellTiter-Blue resazurin reduction assay, CellTiter-Blue was diluted 1:10 into DMEM + 10% FBS and mixed, then media removed from wells of the plate and replaced with the media containing the assay reagent. Plates were then incubated for 3 hours in the dark at 37^{o}C, 5% CO_2, before fluorescence was read directly from the plate using a Cytation 3 cell imaging multi-mode plate reader (Biotek, courtesy of the Optima CDT programme) at 585nm, using an emission wavelength of 550nm and gain set at 50. As with the MTT assay, the background signal from three control wells containing 100 µL DMEM + 10% FBS + 10% CellTiter-Blue was subtracted from each reading.

2.4 | Measurement of confluence

96 well plates were imaged using the IncuCyte© Zoom microscope (Essen Bioscience), taking four images per well at 10X objective. A sample of these images was taken as an image collection, and using IncuCyte© Zoom software, phase contrast, object size filters and hole filling were adjusted to maximise accuracy of cell detection. This processing definition was then applied to every image, with a confluence of each well found from the mean of the confluence values for each of the four images per well.

2.5 | 24-well plate CWR22PC assays testing androgen response

Cells were trypsinised for 90 seconds with 0.05% trypsin + EDTA (Gibco), then centrifuged for 5 minutes at 200 x *g*, before resuspension and manual counting with trypan blue exclusion (Life Technologies) using a FastRead 102 disposable counting chamber (Immune Systems Ltd). Cells were then seeded in a 24-well plate at a density of 5000 cells per well. The following day, media was aspirated and the wells washed with PBS before application of new media containing the treatment conditions, which could contain charcoal-stripped serum (Life Technologies), 1 nM 5α-dihydrotestosterone (Sigma-Aldrich) and/ or 1 µM enzalutamide (MDV3100), (supplied by the Memorial Sloan Kettering Cancer Centre, New York). MDV was stored at 2 mM dissolved in 100% DMSO, and diluted 1:20 to 100 µM in serum-free DMEM before adding to the treatment conditions. DMSO diluted 1:20 in serum free DMEM was added at the same volume to conditions not containing enzalutamide. After a further 3 days media was changed again, using freshly made treatment for the conditions containing enzalutamide. 5 days after treatment total viability of each well was measured by MTT assay, as described above. 75 µL DMSO was added to each well, and after shaking the contents were transferred to a flat-bottomed 96-well optical plate (ThermoFisher) for reading.

2.6 | Seeding density experiments

Cells were trypsinised using 0.05% Trypsin + EDTA (Gibco), centrifuged at 200xg for 5 minutes, and counted using a Countess II automated cell counter (ThermoFisher) using trypan blue (Life Technolgies) exclusion. Cell suspensions (200 µL) of the two starting concentrations were added to column 2 of a 96 well TC-treated flat-bottomed microplate (Corning), three replicates of each. PBS (100 µL) was added to the outer wells (column 1, 12; rows A, H) to prevent evaporation effects, and 100 µL DMEM + 10% FBS +1% PS added to other wells. A twofold serial dilution was then performed, transferring 100 µL cell suspension into the next column, mixing, and repeating into the next column. A plate map of final seeding densities is displayed in Figure 4. The plate was then imaged with an IncuCyte® Zoom (Essen Bioscience) microscope at 37°C 5% CO_2 for 5 days, taking 4 images per well at 10X magnification per well every 1 hour or 3 hours. Images were analysed using IncuCyte Zoom® software to yield confluence data.

	1	2	3	4	5	6	7	8	9	10	11	12
A		CWR22PC					5GSH-6943#5					
B		12000	6000	3000	1500	750	12000	6000	3000	1500	750	
C		12000	6000	3000	1500	750	12000	6000	3000	1500	750	
D		12000	6000	3000	1500	750	12000	6000	3000	1500	750	
E		8000	4000	2000	1000	500	8000	4000	2000	1000	500	
F		8000	4000	2000	1000	500	8000	4000	2000	1000	500	
G		8000	4000	2000	1000	500	8000	4000	2000	1000	500	
H												

Figure 4: Plate map of cell seeding density serial dilution. Values indicate number of cells seeded per well in 96-well plate, seeded in 100 µL media per well. Outer wells (light blue) filled with 100 µL PBS. Seeding densities displayed for CWR22PC and 5GSH-6943#5, but experiments did not necessarily include both on a single plate.

2.7 | Dose response experiments

5GSH-6943#5 cells were seeded at 1500 cells/well in 90 µL, in 96-well plates. After overnight incubation, a range of doses from 100 µM to approximately 100 nM of enzalutamide were prepared by threefold serial dilution in a round bottomed 96 well plate, dissolved in DMEM + 10% FBS + 1% PS + 0.5% DMSO. An additional control well containing no drug was also included. Enzalutamide-containing media (10 µL) from the serial dilution was then applied to the cells to yield a range of concentrations from 10 µM to approximately 10 nM across the plate. A plate map showing enzalutamide concentrations in the experiment is shown in Figure 5. Three days after initial treatment, all media was aspirated and replaced by repeating this process. After a further two days (five days after initial treatment), total cell viability in each well was measured by use of the MTT assay, using 100 µL DMSO per well and reading directly from the Corning 96-well plate.

	1	2	3	4	5	6	7	8	9	10	11	12
A												
B												
C			10 µM	3.33 µM	1.11 µM	0.37 µM	0.12 µM	0.04 µM	0.01 µM	0 µM		
D			10 µM	3.33 µM	1.11 µM	0.37 µM	0.12 µM	0.04 µM	0.01 µM	0 µM		
E			10 µM	3.33 µM	1.11 µM	0.37 µM	0.12 µM	0.04 µM	0.01 µM	0 µM		
F												
G												
H												

Figure 5: Plate map of 5GSH-6943#5 dose response experiments. Final concentrations of enzalutamide shown: prepared at 10x higher concentration by threefold serial dilution and 10 µL added to 90 µL media on the plate. Other wells filled with 100 µL PBS

2.8 | Conditioned media experiments

Human primary bone marrow MSCs in 75 cm^2 flasks at minimum 80% confluency were washed with 15 mL PBS, and 12 mL new DMEM + 10% FBS + 1% PS then added to the flask. After incubation for 24 hours, media was collected and centrifuged at 200 x *g* for 5 minutes, then supernatant passed through a 0.22 µM filter to remove cells, before storage at 4^{o}C. Assay conditions were then prepared the same day as conditioned media was collected. Conditioned media was diluted by 11/30 in fresh DMEM + 11% FBS or 11% CSS, and enzalutamide and DHT added as appropriate to concentrations of 1.1 µM and 1.1 nM respectively. DMSO was added as previously described to conditions not containing enzalutamide. CWR22PC_GB_22 cells were seeded at 7000 per well and CWR22PC_GB_02 and 06 clones at 8000 per well in a 96-well plate (Corning) and the outer wells filled with 100 µL PBS. Two days later, 90 µL of media was aspirated per well and cells then washed with 150 µL serum free DMEM, gently with a manual pipette to avoid loss of cells. After three days all media was removed from the well and replaced with 100 µL new media made up to final concentrations. The same conditioned media used at day 0 was reapplied at day 3, stored at 4°C in the interim period. Five days after initial treatment, images were taken of each well with the IncuCyte Zoom® microscope before performance of either a CellTiterBlue (Promega) or MTT (Sigma-Aldrich) assay.

For testing 5GSH-6943#5 CM response, two 1/15 dilutions of C3H10T1/2 cells were cultured for two days, then media removed, cells washed with 10 mL PBS, and 12 mL BME + 1% sodium pyruvate + 1% L-glutamine + 1% PS with either 10% CSS or 10% FBS was added. On the same day, 5GSH-6943#5 cells were seeded in 96-well plates. After 24 hours, conditioned media was taken from the flask, centrifuged at 200 x *g* for 5 minutes and filtered at 0.22 µM to remove cells. Assay conditions were prepared the same day: conditioned media was diluted 1:2 with DMEM + 10% FBS or 10% CSS before adding enzalutamide or DHT to 1 µM or 1 nM respectively; for conditions without conditioned media, BME + 1% sodium pyruvate + 1% L-glutamine + 1% PS with either 10% CSS or 10% FBS was added to DMEM + either 10% FBS or CSS at a 1:2 ratio. Media was aspirated from the plate with a manual multichannel pipette and washed with 200 µL PBS. New media was added one column at a time using a single Gilson pipette. Media was changed using fresh conditioned media at day 3 with conditions prepared in the same way. Plates were read for confluence data and MTT assay at day 5.

2.9 | Reproducibility/ Min-Max signal experiments

Cells were seeded in the inner 60 wells of 96-well plates (Corning) at the same density as previous 96-well experiments. After one day (5GSH-6943#5 cells) or two days (CWR22PC cells), media was changed and, after a PBS wash, the maximum and minimum control media added in alternating 6-well columns across the plate, as shown in Figure 6. For androgen deprivation min-max experiments, media containing 10% FBS (the maximum control) was compared to 10% FBS + 1µM enzalutamide (CWR22PC cells) or to 10% CSS (5GSH-6943#5 cells). In conditioned media min-max signal experiments, 10% FBS or CSS (the minimum control) was compared to 10% FBS-CM or CSS-CM. Outer wells were filled with 100 µL PBS. Media was changed one column at a time and added using a Gilson single pipette to replicate the protocol of the 96-well conditioned media response assay described above. After either 3 days or 5 days, images were taken with an IncuCyte Zoom® microscope using the scan-on-demand function, and viability read by either MTT or CellTiterBlue assay. For min-max experiments using conditioned media, C3H10T1/2-conditioned media was prepared in the same way as described above.

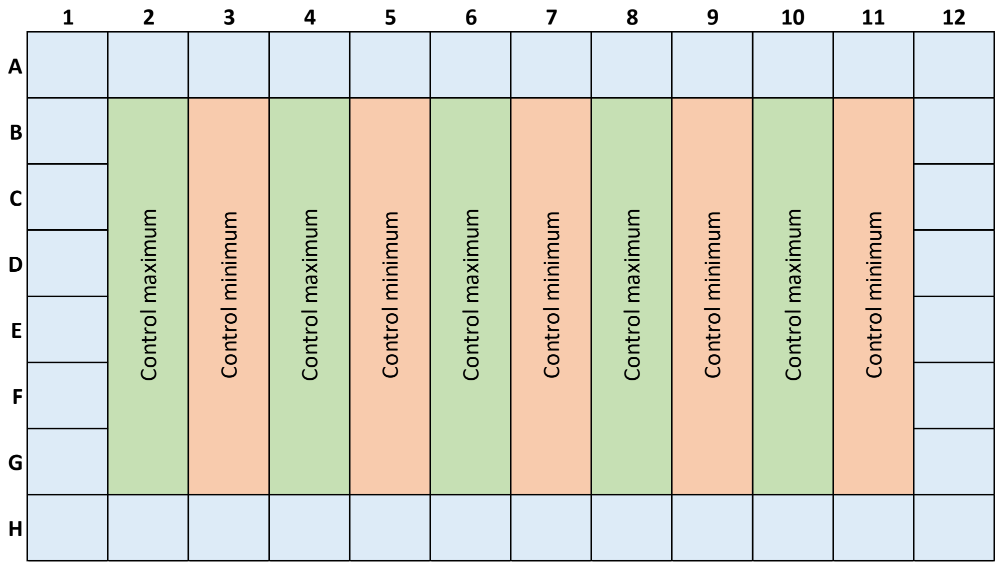

Figure 6: Plate map of Min-Max signal experiments. Alternating columns of two control conditions, 100 µL per well. Outer wells filled with 100 µL PBS.

2.10 | Data analysis

All statistical analysis was performed using Excel 2016 (Microsoft) and Prism 7 (GraphPad Software Inc.). An alpha value of 0.05 was used for all analyses.

For low throughput CWR22PC androgen sensitivity experiments, raw OD values were compiled as grouped data and analysed by paired t-test when comparing two conditions, or by two-way analysis of variance (ANOVA), followed by Dunnett's multiple comparisons test when comparing three or more conditions.

For dose response data, raw OD values for three replicates per concentration tested were normalised to the highest mean, and a nonlinear regression performed using Prism 7, plotting log (enzalutamide concentration) against normalised OD values, using the variable setting. R^2 and IC50 values used were those quoted by Prism 7.

For analysis of CWR22PC_GB_22 response to conditioned media, individual paired t tests were performed for each condition with and without CM between the means of three technical replicates per experiment: each treatment condition (CSS, CSS + DHT, FBS, FBS +

MDV) was considered separately. For individual experiments in the CWR22PC_GB_02 and GB_06 clones, 2-way ANOVAs were performed, comparing the difference between normal and conditioned media for each treatment. Sidak's multiple comparisons test was then performed on these four comparisons.

For analysis of 5GSH-6943#5 response to conditioned media, the mean OD values at 540nm from MTT assays of replicates for the CSS, FBS, CSS-CM and FBS-CM conditions, between the 5GSH-6943#5 conditioned media response assay (without media change at day 3) and the two min-max assays comparing normal media and CM for each serum, were taken and normalised to the mean FBS or CSS value of the three means. A paired t test was then used to calculate the p value, grouping data by the individual experiment performed.

Coefficient of variance (CV) and Z-prime factor (Z') values were calculated for each min-max assay performed. The equations for calculating these values are given below:

$$CV = \frac{\sigma}{\mu}$$

$$Z' = 1 - 3\left(\frac{\sigma_{max} + \sigma_{min}}{\mu_{max} - \mu_{min}}\right)$$

Chapter 3 | Results

3.1 | Human CWR22PC Prostate cancer clones respond to androgen deprivation

Five CWR22PC clones were tested for their response to androgen deprivation in a 5 day, low-throughput 24-well plate assay, quantifying total cell viability by MTT assay. This assay was performed three times and the results displayed in Figure 7. Castrate levels of androgen, achieved by use of media containing 10% charcoal stripped serum (CSS), caused significantly retarded growth compared to fetal bovine serum (FBS) in all clones. In addition, all clones except for CWR22PC_GB_02 were found to have significantly lower growth after 5 days when treated with 1 µM of the second-generation antiandrogen enzalutamide (MDV), although in the CWR22PC_GB_02 clone there was still a strong trend towards decreased growth (P=0.0595). All clones showed a greater negative effect in CSS compared to 1 µM MDV.

The MTT assay yielded negative results in at least some wells of experiments with the CWR22PC_GB_02, 07, and 12 clones when the absorbance of the DMSO background was subtracted. Whilst microscopic inspection revealed that cells stained by MTT were present in these wells, it is likely that the signal from these cells was extremely weak due to low cell number or viability, and thus was not apparent above natural variation in DMSO background readings. Stained cells may have also been inadvertently lost in the washing process before addition of DMSO.

3.2 | CWR22PC prostate cancer cell growth is stimulated by exogenous dihydrotestosterone (DHT)

Further investigation of the androgen responsiveness of CWR22PC clones was conducted by treatment of cells with 1 nM DHT. For the CWR22PC_GB_,07,12 and 25 clones, total viability of cells in a five-day assay was significantly increased by 1 nM DHT in the FBS condition, and trended towards a significance in the CWR22PC_GB_02 clone (P=0.0954). However, 1 nM additional DHT did not increase growth above FBS in the CWR22PC_GB_22 clone, suggesting that the amount of androgen present in FBS is already providing maximal AR-mediated growth response in this clone (Figure 8A). Notably, the decrease in cell viability caused by androgen deprivation was particularly large in this clone (Figure 7), and

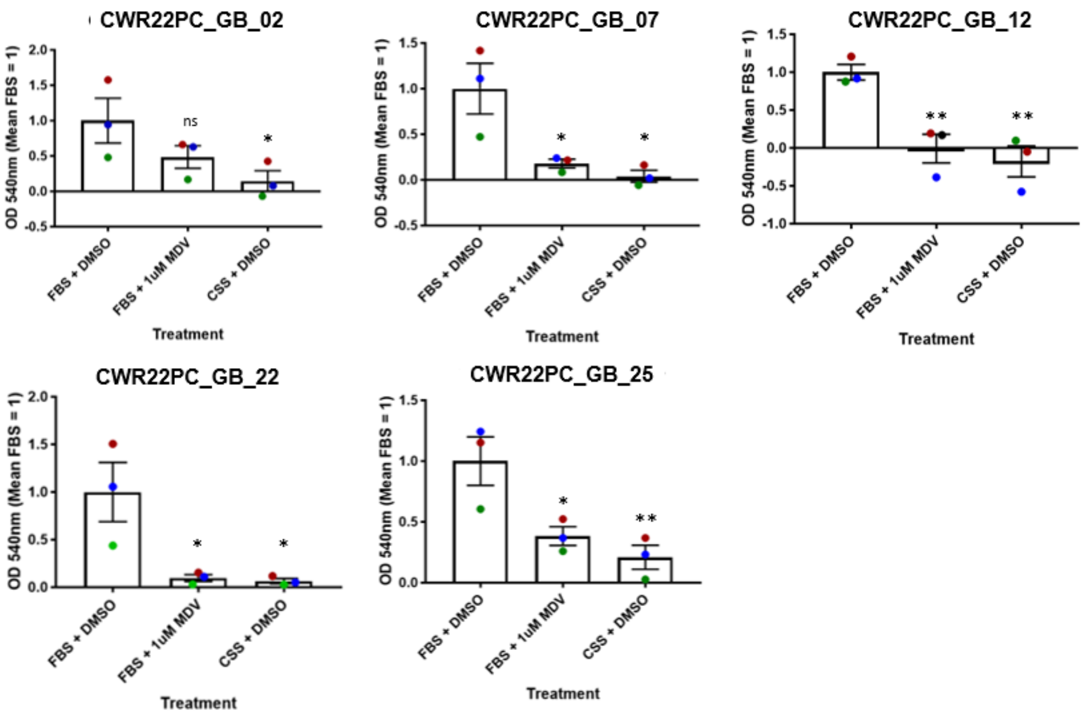

Figure 7: **CWR22PC cell growth is inhibited by androgen deprivation**. 5-day assay in 24-well plate, changing media at day 3. Viability measured by MTT assay, OD 540nm. Data from 3 experiments compared, result from single experiment for a given condition represented by a single point, each colour represents a different experimental repeat (mean of 3 technical replicates). Bars mean of three repeats (each the mean for one experiment) +/- S.E.M. Data normalised to mean FBS value (=1 for each experiment) $P < 0.05$, comparison with FBS + DMSO (One-way ANOVA, Dunnett's multiple comparisons test)

cells of this clone grew faster than others in culture in FBS (data not shown), supporting this possibility.

All clones showed a very strong trend of increasing growth with DHT administration in the CSS condition (Figure 8B). The increase in growth with 1nM DHT is much larger in CSS then in FBS, as expected. However, the effect was only statistically significant in the CWR22PC_GB_25 clone (P= 0.0044), the GB_07 (P=0.0569) and GB_22 (P=0.0705) clones were close to significance. P was equal to 0.1550 and 0.0924 in the GB_02 and GB_12 clones respectively. The reason why P>0.05 in these clones was likely due to high variation in the magnitude of increase between replicate experiments; nevertheless, 1nM DHT clearly has a large effect on viability, and further repeats or optimisation to improve assay consistency and sensitivity would likely reveal this to be statistically significant. 1 nM DHT rescues CWR22PC cell growth in CSS to a similar level to the FBS + DHT condition (data not shown), indicating that androgen removal from CSS is responsible for the decrease in cell growth: the difference in total cell viability between the CSS and CSS + DHT conditions should indicate the maximal effect of AR signalling on the growth of the clone. However, in the CWR22PC_GB_07,12 and 22 clones, total viability was lower in CSS supplemented with DHT compared to FBS supplemented with DHT (data not shown), suggesting the reduced growth in CSS is due in part to loss of other factors. As 1nM DHT should be a saturating dose, and this is seen in the CWR22PC_GB_22 clone which did not respond to additional DHT in FBS, this effect is unlikely to be due to additional androgen in FBS. There appears to be little difference between the FBS + DHT and CSS + DHT conditions in the CWR22PC_GB_02 and 25 clones, however.

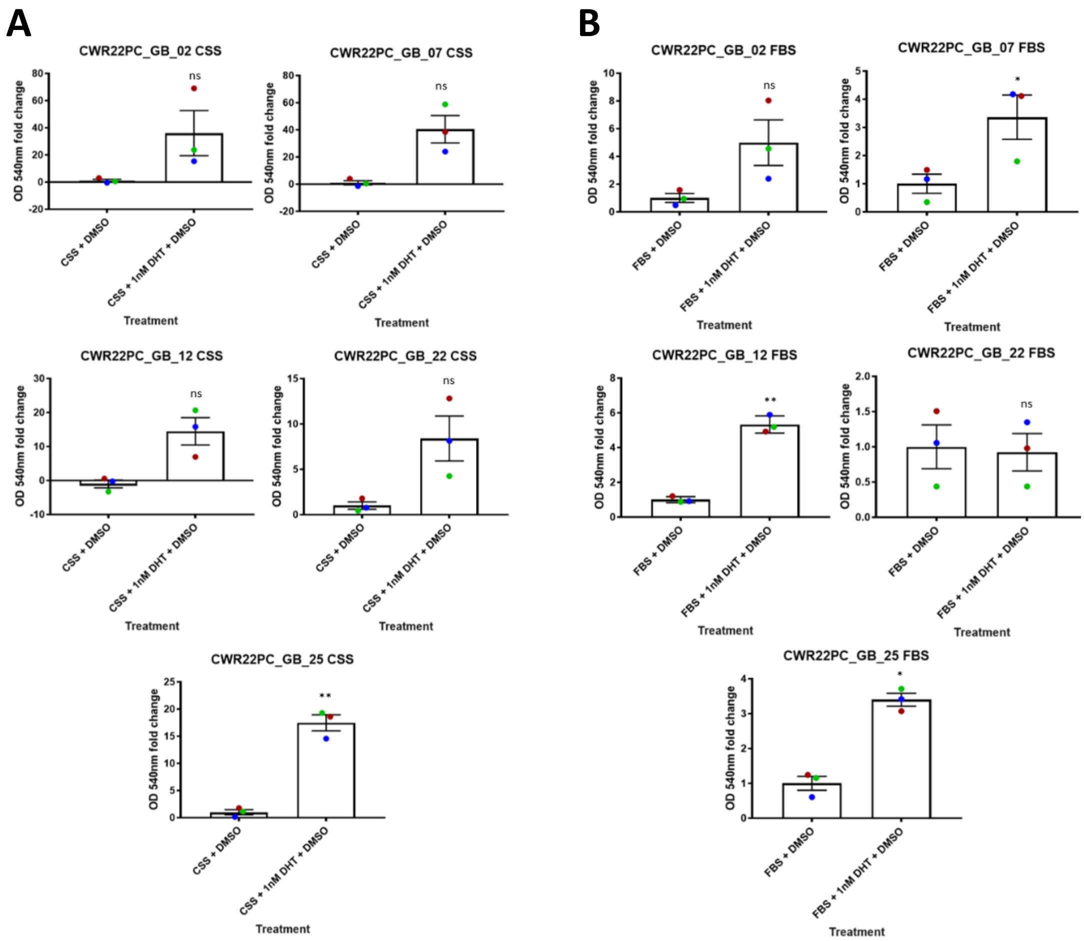

Figure 8: **CWR22PC cell growth is stimulated by androgen administration**. 5-day assay in 24-well plate, changing media at day 3. Viability measured by MTT assay, OD 540nm. **(A)** Difference between FBS and FBS + 1nM DHT; **(B)** Difference between CSS and CSS + DHT. Data mean of 3 replicates from 3 repeat experiments, result from single experiment for a given condition represented by a single point, each repeat experiment represented by a different colour. Bars mean of three repeats values =/- S.E.M. Data normalised to mean FBS (A) or CSS (B) value between 3 experiments (=1 for each experiment). P < 0.05, comparison with either CSS + DMSO or FBS + DMSO (Paired T test).

3.3 | Effects of co-administration of DHT and enzalutamide differ between CWR22PC clones

1 nM DHT and 1 µM enzalutamide were added to cells together to study the effects of AR inhibition on cells stimulated by maximal androgen signalling. As shown in Figure 9, growth rate when both were added was significantly higher than the FBS + MDV condition in the CWR22PC_GB_07 and 22 clones, and trended higher in the CWR22PC_GB_12 clone (P=0.0738); in the CWR22PC_GB_07 and 12 clones FBS + 1 nM DHT + 1 µM MDV also produced a trend of higher growth than FBS alone (P=0.0823 and P=0.1981 respectively), despite the presence of an AR inhibitor. A possible explanation for this is that AR block ade may cause upregulation of the AR allowing response to additional androgen, or that the high concentration of androgen displaced the drug from the AR: enzalutamide has two- to three-fold lower affinity for the AR than DHT [39]. In this case, additional DHT may displace enough MDV to stimulate AR substantially more than the androgen in FBS alone. However, there was no significant increase in cell growth compared to FBS + MDV in the CWR22PC_GB_02 and 25 clones, and enzalutamide significantly decreased viability in the FBS + DHT + MDV condition compared to FBS + DHT alone. However, viability in FBS + DHT + MDV condition was still higher than FBS + MDV, and was at a similar level to the FBS + DMSO condition in both clones. It was not clear why the effects of MDV when administered with 1 nM DHT differed between clones.

3.4 | Murine Myc-CaP Bo prostate cancer cells respond to androgen deprivation

It was also established that the 5GSH-6943#5 clone of the murine prostate cancer cell line MyC-CaP Bo responded to androgen deprivation. Initial experiments revealed only a small response to CSS and enzalutamide compared to FBS alone (Figure 10A). Whilst a relatively small response to enzalutamide concorded with previous experiments in this lab, a much larger effect of CSS was expected. Using different stocks of FBS and CSS did not much change the size of this effect, even after thawing a new frozen vial of 5GSH-6943#5 cells (data not shown). In addition, 1 nM DHT had a negative effect on the growth of cancer cells, as measured by both MTT assay and confluence (representative images shown in Figure 10B). Further testing using different doses of DHT revealed that this effect was not due to the incorrect dose of DHT being given or the DHT stock being at the incorrect concentration: the effect was also seen at 10X lower dose using the same DHT stock as the

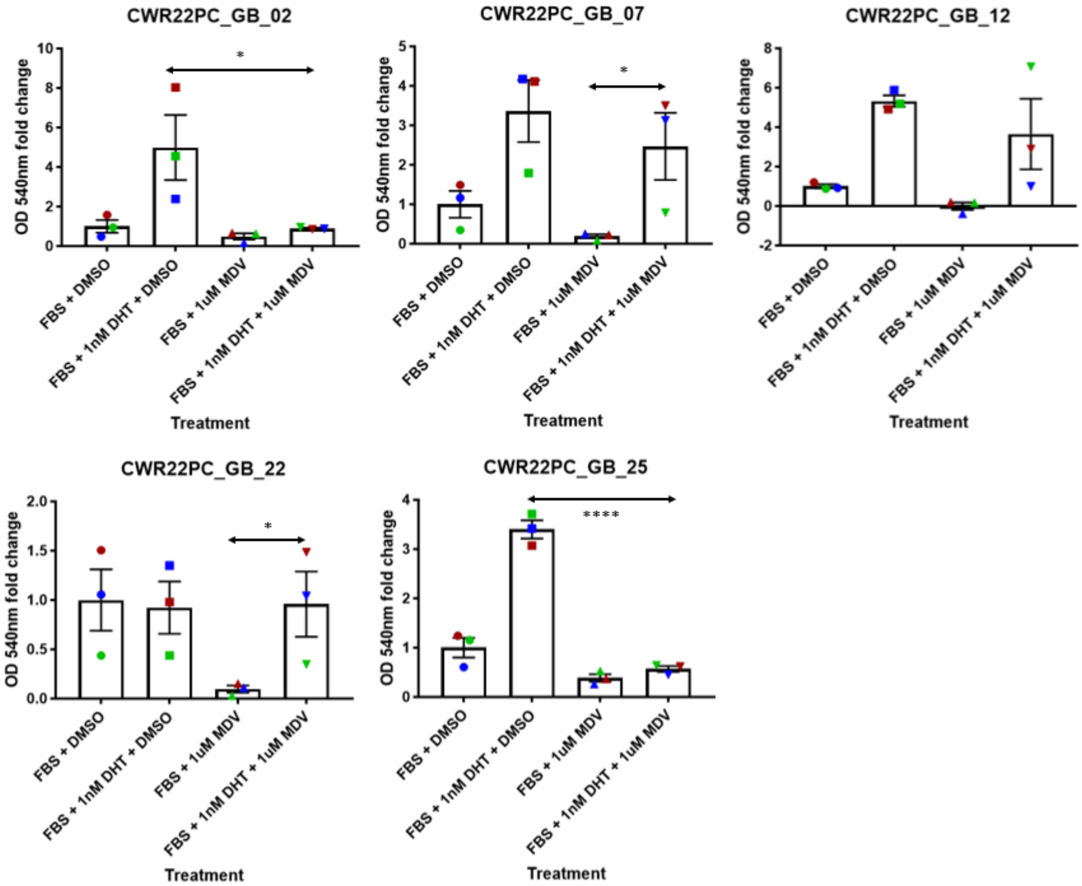

Figure 9: Response of 5GSH-6943 cells to double administration of DHT and MDV. 5-day assay in 24-well plate, changing media at day 3. Viability measured by MTT assay, OD 540nm. Data mean of 3 replicates from 3 repeat experiments, result from single experiment for a given condition represented by a single point, each repeat experiment represented by a different colour. Bars mean of three repeats values +/- S.E.M. Data normalised to mean FBS + DMSO value (normalised to 1). P < 0.05, comparison to FBS + DHT + MDV condition (2-way ANOVA, Dunnett's multiple comparisons test).

previous experiment, and at the same and 10X higher dose using new stock (Figure 10C). It appears that these cells underwent a phenotypic change in response to DHT, appearing smaller and more densely packed than cells treated with the other conditions (Figure 10B). This may have been due to alterations in AR signalling conferring a very different androgen sensitivity on cells: different 5GSH-6943#5 cells used later did not perform in this way. Closer examination of these cells revealed mycoplasma infection and cell line contamination, which may have been responsible for this unexpected behaviour.

These cells were replaced with a new 5GSH-6943#5 stock, which underwent antibiotic selection with 1 mg/mL G418 to ensure the appropriate cells were being used. Multiple different FBS stocks were tested against CSS and with MDV treatment to determine the androgen sensitivity of the cells and whether different serum stocks gave different responses: as shown in Figure 10D, growth rate was slightly higher in the FBS stock of the lab of Professor Jeffrey Pollard than FBS used for other experiments in this project stored at -20°C or -80°C. Enzalutamide treatment reduced viability to a similar level in all FBS stocks: by 23% and 21% in the -20°C and -80°C FBS respectively, and by 37% in the FBS of the neighbouring lab. Faster growth in the Pollard lab FBS was thus androgen dependent, likely due to increased concentration of androgen. A stronger ADT response was seen in charcoal-stripped serum reducing viability by 60%, 61% and 67% compared to the -20°C, -80°C and Pollard lab sera respectively. Whilst the greatest effect size was seen using FBS from the Pollard lab, a lack of availability of this serum meant that instead the FBS kept at -80°C was used for subsequent experiments in 5GSH-6943#5 cells. The new 5GSH-6943#5 cells also responded positively to androgen replacement by 1nM DHT in the CSS condition, although viability was still substantially lower than in FBS alone.

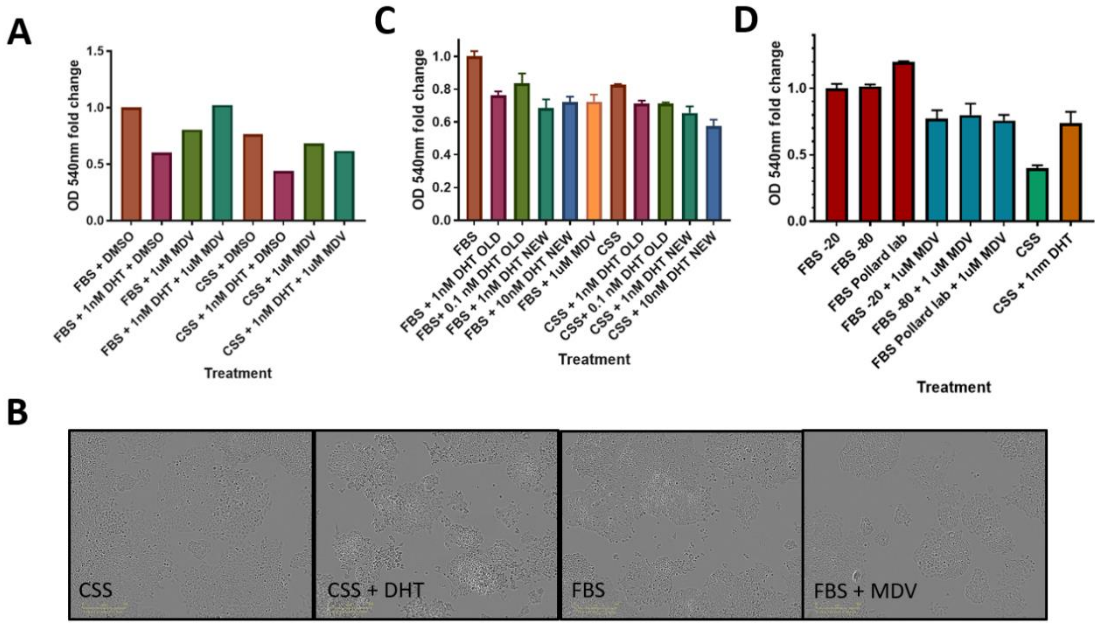

Figure 10: Response of 5GSH-6943#5 murine prostate cancer cells to androgen deprivation. **(A)** 5-day MTT assay single experiment in 12 well plate (5000 cells/ well seeded) of 5GSH-6943#5 cells under various conditions of androgen supplementation and deprivation (OD 540nm, normalised to FBS value). **(B)** Representative images from 96-well 5GSH-6943#5 experiment, using same batch of cells as in (A) and (C). 10X objective, taken at day 5 with IncuCyte Zoom® **(C)** 96-well MTT experiment testing dose of DHT on 5GSH-6943#5 cells. Seeded 1000 cells/ well, OD 540 nm (normalised to FBS) +/- S.E.M (3 replicates each condition). **(D)** 5-day experiment, 500 cells/ well seeded in 24-well plate. MTT assay of growth response to androgen deprivation and different batches FBS. OD 540nm normalised to FBS -20°C +/- S.E.M. (3 replicates)

3.5 | Optimisation of cell density

Miniaturisation of this low-throughput assay onto a 96 well plate required the optimal cell seeding density per well to be elucidated. To find this, a twofold serial dilution was performed to achieve a range of cell densities on a 96 well plate, and confluence was measured at sequential time points for five days using the IncuCyte Zoom® microscope (Figure 11). The appropriate number of cells to seed for a five-day assay could be determined by identification of trace approaching reasonably high levels of confluence by 5 days whilst remaining in logarithmic growth phase and growth not slowing due to contact inhibition (shown by a decrease in the slope of the curve, for example in Figure 11E). Plates were not kept incubated in this experiment for more than 5 days due to nutrient depletion and waste product generation in the media, thus extrapolation of the curve a further 24 or 48 hours is required, as cells were seeded one or two days before treatment. Furthermore, as subsequent assays would utilise a 10% FBS + DHT condition, cell densities selected would need to allow room to account for the higher growth rate with additional androgen.

For the CWR22PC_GB_02, 06 and 07 cell lines, confluence remained low even after 5 days (Figure 11A, B, C). For these cell lines, a density of 8000 cells was chosen: this was adjusted to 7000 cells/well for the faster growing CWR22PC_GB_22 clone (Figure 11D). Whilst this meant that confluence was still quite low at the end of the experiment, seeding densities of 10000 and above had too high a starting confluence, and may have been affected by too much cell-cell contact at early stages of the experiment. Furthermore, the ratio of increase in confluence over the 5-day period was found to be the same or even larger at 8000 cells seeded compared to 12000 (Table 1). Low final confluence values in DMEM + 10% FBS for CWR22PC_GB_02,06 and 07 also left room for confluence to be considerably increased by supplementation with 1 nM DHT without cells becoming overconfluent. The 5GSH cells grew much faster and a lower cell density was required: due to an overlap in traces at the between the 1000 and 750 densities (Figure 11E), the experiment was repeated with cell densities of 1000, 750 and 500 (Figure. 11F), from which an appropriate starting density of 500 cells per well was chosen.

	CWR22PC_GB_02	CWR22PC_GB_06	CWR22PC_GB_07	CWR22PC_GB_22
12000 cells/ well	2.29	2.31	1.76	2.56
8000 cells/ well	2.25	3.22	1.88	3.02

Table 1. Ratio of change in confluence (mean of confluence from 3 replicate wells) over 5 days between beginning and end of seeding density experiment (first and last data points) between the 12000 and 8000 – cell seeding densities.

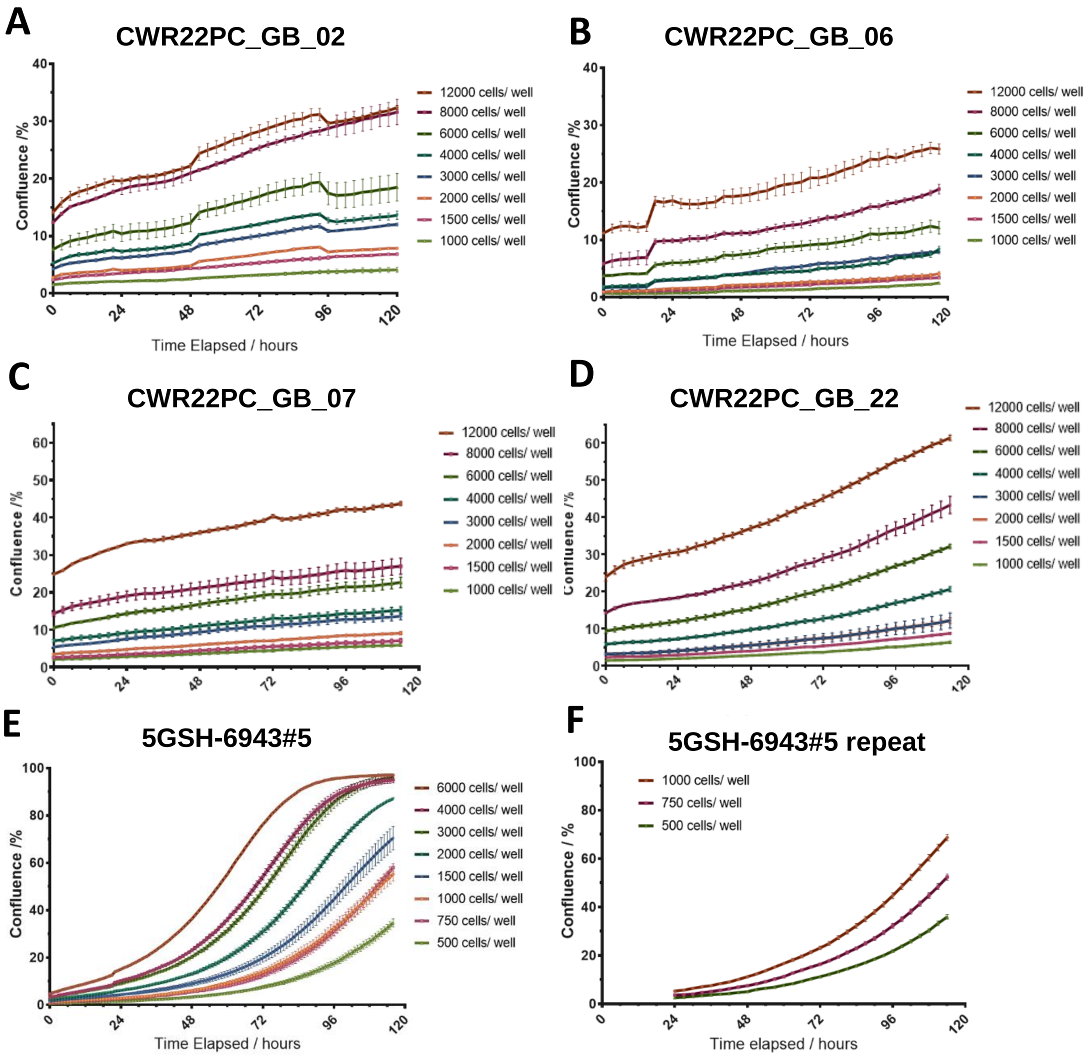

Figure 11. **96 well plate experiments to elucidate optimal seeding density in various cell types**. Achieved by twofold serial dilution of cells seeded across the plate. Four 10X images taken per well using an IncuCyte Zoom® microscope. **(A – D)** CWR22PC_GB_02,06,07,22 clones, images taken every 3 hours. **(E, F)** 5GSH-6943#5 cells, images taken every hour Cells imaged from immediately after seeding with exception of (F), where imaged 24 hours later. Overlapping data in (E) necessitated a repeat of the experiment for the lowest cell densities (F). Depicted mean of three replicates (each the mean confluence of four images per well) ± S.E.M.

3.6 | Determination of optimal dose of enzalutamide for murine experiments

For experiments using CWR22PC cells, a dose of 1µM enzalutamide was used for high throughput experiments: this had already been shown to produce a strong response in 24 well plate experiments (Figure 7). For 5GSH-6943#5 cells, dose response experiments were carried out varying MDV dose by threefold serial dilution. From these data (Figure 12), there is little response to MDV below 0.3 µM MDV, where viability falls steeply, then steadily decreasing as MDV3100 concentration rose further. The IC50 for the dose response curve was calculated to be 5.9 µM, however, 1 µM was still chosen: it is more in line with other publications and considered more relevant to the treatment dose *in vivo* [15,45] and still fairly close to the IC50, considering dose was varied on a log scale. This data ideally would have been repeated to achieve a more reliable measure of IC50. Nevertheless, a dose of 1 µM MDV in this experiment produces a decrease of around 30%, in line with other experiments using this cell line in this investigation (Figure 10D).

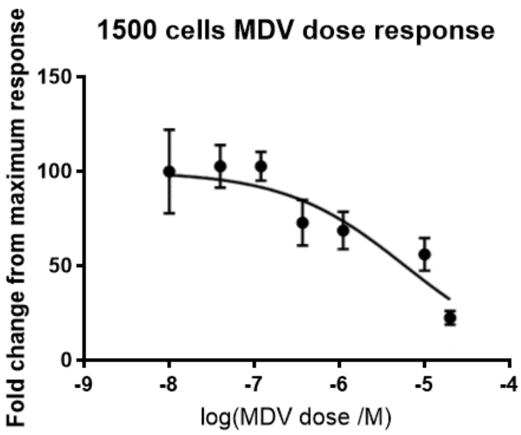

Figure 12. Determination of optimal dose of MDV for murine prostate cancer cell experiments. Dose response of 5GSH-6943#5 cells to enzalutamide (MDV3100) measured by MTT assay after 5 days. Seeding 1500 cells per well in 96 well plate, media replaced after 3 days. OD 540nm, data normalised to highest mean value (=100). Mean of three replicates +/- SEM. IC50=5.9x10^{-6} M. R^2 = 0.7823

3.7 | Optimisation of CellTiter-Blue incubation time

To ascertain the amount of time needed to incubate cells for assays using CellTiter-Blue, 10 µL CellTiter-Blue was added to each 100 µL well on day 5 of a 96-well plate androgen deprivation assay using CWR22PC_GB_02 and 22 cells. The plate was then incubated in the dark at 37°C and 5% CO_2. Fluorescence was measured at 585nm after exciting at 550nm, at 90 minutes, 180 minutes and 360 minutes after CellTiter-Blue addition. The plate was then stored in the dark overnight at room temperature, then read again 24 hours after CellTiter-Blue addition. In both clones, there were slightly larger differences between conditions after 3 hours compared to 90 minutes; differences after 6 hours were either equal or slightly lower than at 3 hours (Figure 13). The 24-hour timepoint showed a reduction in the difference between conditions due to the exhaustion of all CellTiter-Blue present in some wells (data not shown). Based on this data, an incubation time of three hours was chosen for subsequent conditioned media response and min-max experiments using CellTiter-Blue.

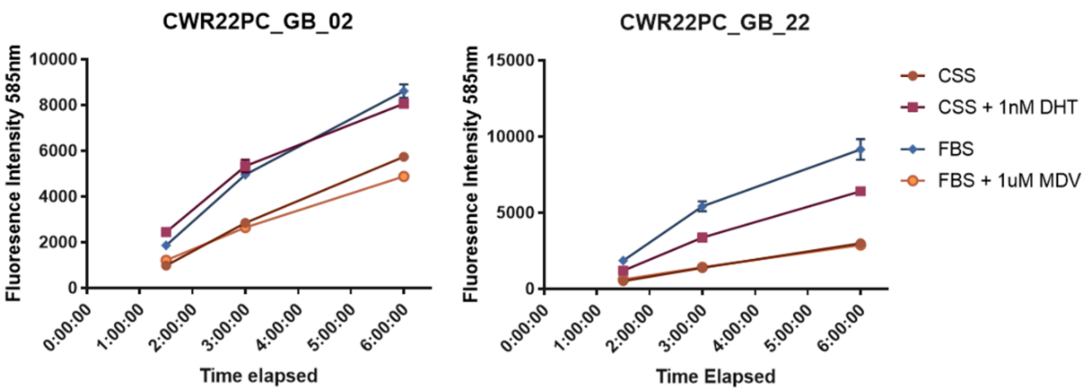

Figure 13. Determination of optimal time of incubation for CellTiter-Blue assay. Cells seeded at 8000 (CWR22PC_GB_02) or 7000 (CWR22PC_GB_22) cells per well and treated 2 days later; media then changed at day 3. 10 µL CellTiter-Blue added with automatic multichannel pipette directly to the treatment media at 5 days. Fluorescence read with excitation at 550nm, emission at 585nm. Readings after 90 minutes, 180 minutes and 360 minutes at 37°C and 5% CO_2. Mean fluorescence intensity (of 3 replicate wells)) +/- S.E.M. CSS and FBS + 1 µM MDV traces for CWR22PC_GB_22 clones overlaid upon eachother.

3.8 | Response of CWR22PC cells to MSC-conditioned media.

Five-day 96 well assays were performed using human bone marrow MSC (BM-MSC)-conditioned media to investigate whether secreted factors from MSCs affect prostate cancer cell growth with and without androgen deprivation. Figure 14A shows the combined results of three replicate experiments using 1:2 diluted MSC-conditioned medium on CWR22PC_GB_22 cells for 5 days. Media was changed at day 3, using the same CM that had been used at day 0 (stored in the interim at 4°C). As conditioned media could only be prepared in FBS, CSS conditions contained 6.7% CSS and 3.3% FBS. Individual two-way ANOVA analyses of the effect of CM on total viability for each condition did not reveal a significant difference in any of the 4 conditions, however the increase in viability with conditioned media in FBS + 1 µM MDV trended towards significance (P=0.1045). The effect of conditioned medium was small, increasing viability by 36% in the FBS + MDV condition, and much smaller rises in FBS and CSS. The markedly higher effect in FBS + MDV than CSS, was likely due to the presence of FBS in the CSS condition: compared to the FBS condition, proliferation was impaired much less compared to FBS + MDV (by roughly 35% and 75% respectively). Notably, conditioned media had a negative effect on cell number in the CSS + 1 nM DHT condition, despite viability in CSS + DHT being no higher than in FBS.

Due to constraints of time and the cells used it was not possible to complete three biological replicates for the other CWR22PC clones. However, preliminary experiments were performed using the CWR22PC_GB_02 and CWR22PC_GB_06 clones (Figure 14B, C). Neither clone responded as greatly to 1 µM enzalutamide as the CWR22PC_GB_22 cells, however, both clones showed a greater response to BM-MSC conditioned media: similarly, the positive effect was proportionally greatest in the FBS + MDV condition (72% and 96% in the GB_02 and GB_06 clones respectively). A two-way ANOVA between the three replicate wells, comparing normal media to CM for all conditions (using Sidak's correction for multiple comparisons) showed a significant ($P<0.05$) increase in all conditions bar CSS+DHT in CWR22PC_GB_06 cells. In the CWR22PC_GB_02 clone, there was a significant increase in the CSS and FBS + MDV treatments, with a trend towards significance in the FBS condition. However, as this analysis was performed using data from only one experiment, it is not correct to say that a significance response to CM has been identified.

Data was collected using both CellTiter-Blue and MTT assays in this experiment, and by confluence measurement with the IncuCyte Zoom®. MTT was the more sensitive assay, giving proportionally larger differences than CellTiter-Blue between conditions. The MTT data also concorded much more closely to the confluence values, suggesting that the MTT assay results were more representative of the actual total cell number (Figure 14D). Later min-max experiments, comparing alternate rows of control and treatment replicates over a whole plate, would confirm a smaller effect size when using CellTiter-Blue.

3.9 | Determination of optimal assay protocol in CWR22PC cells

It is preferable to avoid changing growth media during an in vitro assay if possible, as it may cause loss of cells, changing concentrations of compounds within the media and disruption of other conditions affecting growth, such as temperature and pH. This could be achieved by reducing the length of the assay or by conducting the assay for five days without media replacement. Use of the IncuCyte Zoom® to monitor confluence in cells undergoing androgen deprivation shows that the majority of the response of CWR22PC cells to enzalutamide occurs after day 3 (Figure 15). Confluence clearly starts levelling off between 48 and 72 hours in both the 10% FBS + MDV and 10% CSS traces, after which it begins to fall in the enzalutamide (MDV)-treated condition and no longer increases in the CSS condition.

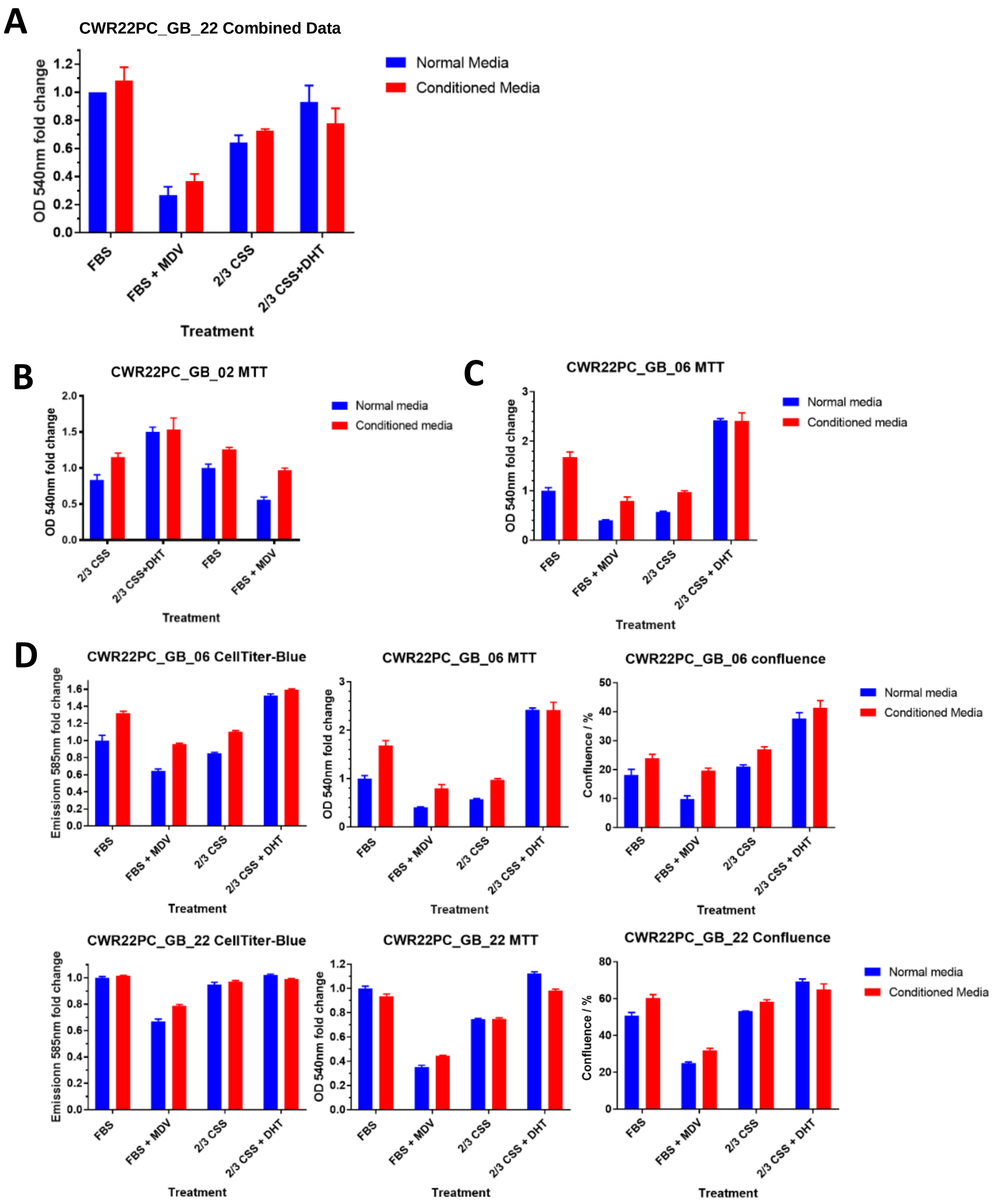

Figure 14. CWR22PC cell growth is stimulated by bone marrow MSC – conditioned media. (A) Combined data from three 5-day 96-well experiments on CWR22PC_GB_22 cells (seeded 7000 cells/well), read by MTT assay. Means of three technical replicates taken and normalised to mean FBS value (=1), then data from three biological replicates combined. Normalised OD 540nm +/- S.E.M. **(B, C)** Single experiments in CWR22PC_GB_02, and _06 clones: 5 day 96-well experiment, seeded 8000 cells/well. Mean of 3 replicate wells MTT signal OD 540nm normalised to mean FBS value +/- S.E.M **(D)** Comparison of CellTiter-Blue and MTT assays, and confluence data obtained from IncuCyte Zoom® microscope, read from same 96 well plate for CM experiment on two CWR22PC clones. All three readings taken sequentially from the same plate. Data for MTT and CellTiter-Blue assays normalised to mean FBS value, all data =/- S.E.M.

The downward drop at 72 hours (particularly in the 10% FBS + MDV trace) is likely due to mechanical loss of cells during media replacement. Confluence in the CSS trace is likely lower due to loss of cells during the media changing process, however the effect of CSS in reducing cell proliferation can still be seen. These results suggested that a 3-day assay was not viable for this investigation, which was confirmed by later min-max assays.

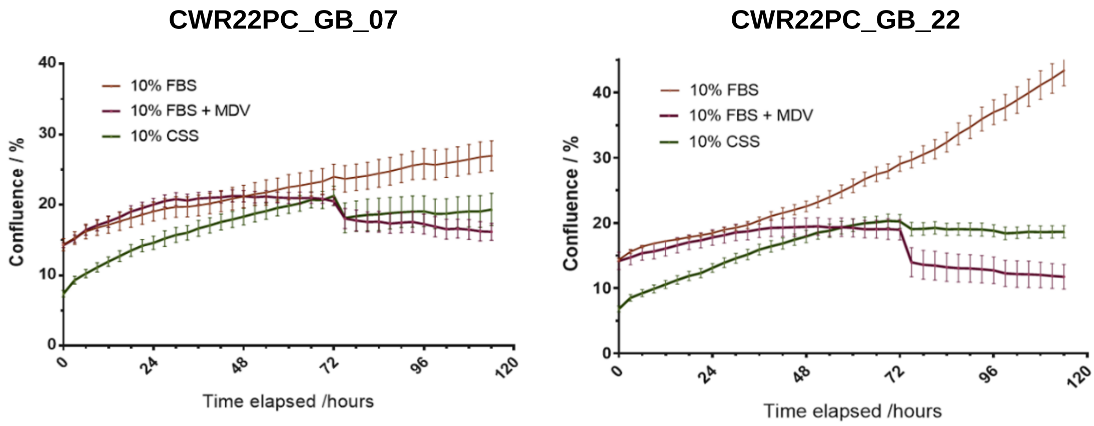

Figure 15. Most of response to androgen deprivation in CWR22PC cells occurs after day 3. 5 day 96-well plate experiment investigating effects of enzalutamide (MDV) and charcoal stripped serum (CSS) over time. Cells seeded at 8000 per well in DMEM + 10% FBS; media changed in FBS + MDV and CSS conditions after 4 hours and after 3 days. Four images per well taken at 10X objective with an IncuCyte Zoom ® microscope. Error bars +/- S.E.M.

To investigate whether the media change at day 3 could be omitted, during experiments testing the response of CWR22PC clones to androgen deprivation and MSC conditioned media, assays were performed with and without this media change (Figure 16). When media was changed on day 3, the same conditioned media as used on day 0 was used, stored at 4°C in the interim. Omission of the media change did not reduce the ability of the assay to discern differences between these conditions for either the CWR22PC_GB_06 or GB_22 clones. In fact, a slightly greater CM effect in FBS + 1 µM MDV was seen when the media was not changed (Figure 16, Table 2). Also, monitoring of CWR22PC cells seeded at the same densities for five days without a media change did not show any indication of reduced growth rate due to nutrient starvation (Figure 11). Changing the media at day 3, if using the same CM at day 3 than at day 0, was thus unnecessary for this assay. It is possible, however, that a greater effect of conditioned media could be obtained if, when changing media at day 3, freshly obtained conditioned media is used. This was found to be the case in 5GSH-6943#5 cells, as described below (Figure 17). However, due to the constraints of the slow growth rate of the primary human BM-MSCs, this investigation could not be performed within the timeframe of this project.

	FBS / FBS+ MDV	CM/NM (FBS + MDV)
CWR22PC_GB_06		
Media Change Day 3	2.45	1.96
No Media Change	5.29	2.14
CWR22PC_GB_22		
Media Change Day 3	2.83	1.26
No Media Change	3.95	1.33

Table 2. Proportional differences between FBS and FBS + MDV and between FBS + MDV and FBS + MDV CM conditions in the assay shown in figure 16, with or without media replacement (using the same conditioned media as before stored at 4oC) at day 3 of the 5-day assay.

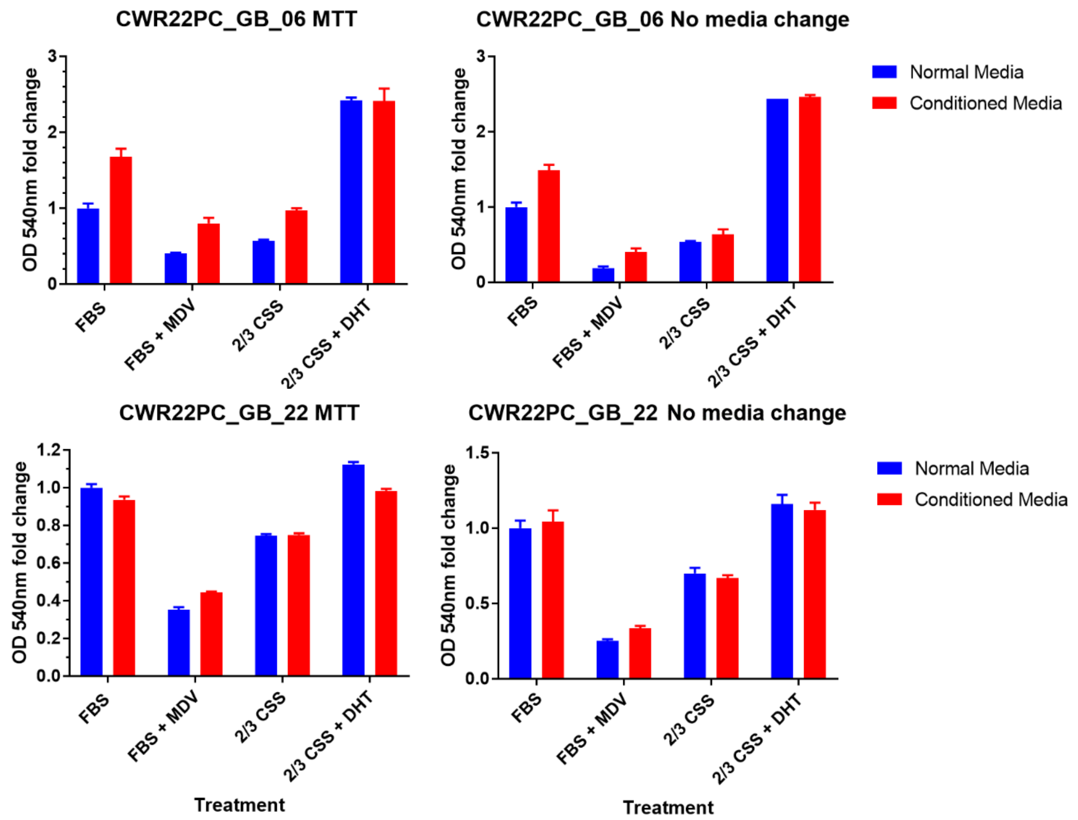

Figure 16. Omission of media change at day 3 does not affect response to conditioned media. 96-well assay 5 day in CWR22PC_GB_06 and CWR22PC_GB_22 clones showing total cell viability as measured by MTT assay in response to androgen deprivation (by CSS or MDV) and MSC conditioned media. Conditioned media contained 10% FBS before conditioning with mesenchymal stem cells for 24 hours, then diluted 1:2 into normal media to give treatment condition. Therefore, to control, all CSS conditions contain 1/3 either standard DMEM + 10% FBS or MSC-conditioned DMEM +10% FBS. Mean OD 540nm of 3 replicate wells normalised to mean FBS value +/- S.E.M of 3 replicates.

3.10 | 5GSH-6943#5 cells to MSC conditioned media under androgen deprivation conditions

5-day high throughput experiments were also performed to test the response of 5GSH-6943#5 cells to CM of the C3H10T1/2 murine MSC line. Unlike the primary human MSCs, C3H10T1/2 cells were capable of growth in media containing charcoal-stripped serum, thus CSS conditions contained 100% CSS. This assay was performed both with and without a media change on the third day, using freshly obtained C3H10T1/2 CM (Figure 17).

Comparing 3 replicate wells of each condition in this single experiment, only in the CSS condition did MSC-conditioned medium cause a significant increase in total viability both with and without a media change (P= 0.0046 and 0.0347 respectively, 2-way ANOVA comparing CM to normal media for all conditions, with Sidak's correction for multiple comparisons). The positive effect of CM in FBS + 1 µM MDV without a media change and the negative effect in the FBS condition when media was changed on day 3 were also significant by this analysis. However, as with the CWR22PC data, we cannot assert a significant effect of C3H10T1/2 CM on this cell line, as doing so would require analysis of at least three repeated experiments. From these data, it appears that MSC-conditioned media only has a particularly substantial positive effect on 5GSH-6943#5 cell growth at castrate levels of androgen (i.e. in CSS). However, there was an increase in the CSS + DHT condition which trended towards significance (P=0.0605) when media was changed at day 3, in contrast to the decrease in growth in CWR22PC cells (Figure 14). When new media was applied at day 3 there was a greater increase in cell growth in the CSS condition caused by conditioned media than when there was no media change, although the difference was fairly small (61% with fresh CM at day 3, compared to 47% with no media change). A greater reduction in growth in CSS compared to FBS was also seen when the media was changed at day 3.

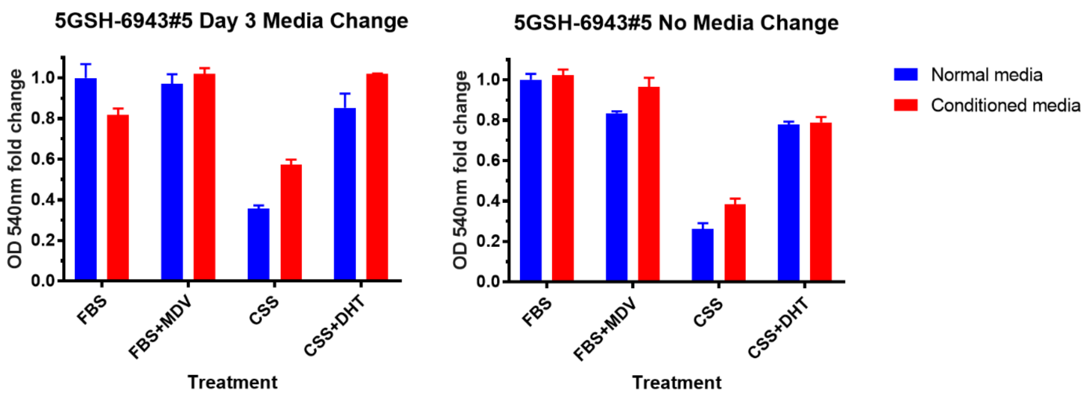

Figure 17. 5GSH-6943#5 response to C3H10T1/2 conditioned medium. 5-day assay in 96 well plate, with/ without media change at day 3 using fresh C3H10T1/2-conditioned media. Total viability of well measured by MTT assay, OD 540nm mean of three replicates normalised to mean FBS value +/- S.E.M.

Data for the effect of conditioned media in the CSS and FBS conditions (without the day 3 media change) in the assay in Figure 17 was combined with two min-max assays each comparing the two conditions, to allow for statistical analysis of response conditioned media in these conditions. A paired t-test demonstrates that there is a significant response

(P=0.041) to C3H10T1/2-cell conditioned media in the CSS condition in this cell line (Figure 18A). There was no response to CM in the FBS condition (Figure 18B).

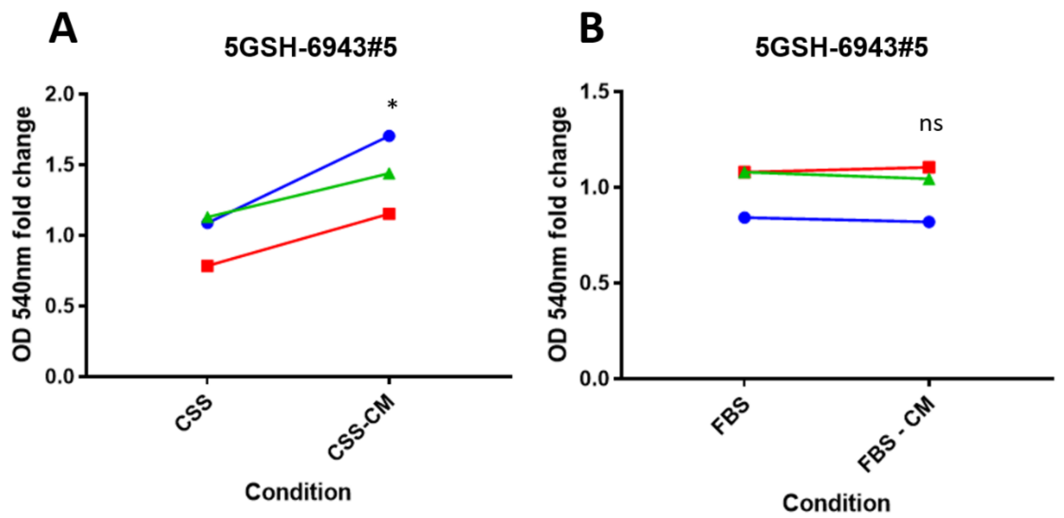

Figure 18: C3H10T1/2 – conditioned media stimulates 5GSH-6943#5 growth in the CSS condition. (A) Response in the CSS condition, MSCs cultured with CSS for CM production. **(B)** Response in the FBS condition, MSCs cultured with FBS from CM production. Data from 3 experiments (one experiment per line), 5-day assay in 96 well plate, no media change at day 3. Mean OD 540nm by MTT assay, normalised to mean CSS/ FBS value between 3 experiments. Paired t test, P<0.05.

3.11 | Assessment of suitability of the CWR22PC_GB_22 clone for high throughput drug screening

Min-max signal variability assays comparing difference in cell growth between FBS and FBS + MDV were undertaken for the CWR22PC_GB_22 clone to determine the signal-to-noise between control and treatment groups, in terms of the assay window and variance of replicates. CWR22PC cells were treated in alternating columns between the two conditions and read by either MTT or CellTiter-Blue assay at day 3 or day 5. Confluence was read using the IncuCyte Zoom® immediately before addition of the viability assay reagent. Media was not subsequently changed during the assay period, as per previous findings (Figure 16). Coefficient of variance and Z’ data is summarised in Table 3. Reading the plate at day 3 did not give a high enough effect size to be suitable for a drug screen by any modality: MTT experiments after 3 days in this clone gave Z’ values indicating a highly marginal assay (0.09 and 0.15), whilst CellTiter-Blue and confluence readings gave negative Z’ values. This was likely mostly due to insufficient effect size at 3 days (compare Figures 19A, 19B). At 5 days, the MTT assay gave Z’ values of 0.74 and 0.40; whilst CellTiter-Blue gave substantially lower Z’ scores of 0.22 and -0.48, indicating a marginal and an unusable assay respectively. The difference in Z' is due to a smaller difference between the means in the CellTiter-Blue assay (Figure 19): CV values were similar between the two assays. As in previous experiments (Figure 14), confluence data (Figure 19C) concorded much closer with the MTT than the CellTiter-Blue assay, suggesting MTT was more representative of total cell number.

The Z' values for confluence at day 5 varied widely, ranging from 0.59 to 0.07: at the higher end, confluence could thus provide an ideal assay for high throughput screening, although for each plate the Z' for the MTT assay was greater. The effect size between the means of the two conditions of the MTT assay (3.59 and 3.51-fold) was larger than that between the confluence values (2.74 and 2.57-fold) read on the same plate. This may be due to enzalutamide inhibition of cell viability, increasing the likelihood of accidental detachment and loss of cells during changing media to add MTT. It is more likely, however, that confluence underestimates the difference between conditions: it is by its nature considerably less sensitive and accurate a measure of cell number than viability assays, and will detect dead or minimally viable cells, possibly causing it to overestimate cell growth in the enzalutamide condition. These experiments therefore demonstrate that the MTT assay is the most suitable measure of cell number for a drug screen based on this assay.

Figure 19D shows data from Figures 19A-C transposed and displayed by rows across the plate, rather than by column. This reveals some drift effects in some plates, chiefly the CellTiter-Blue day 3 plate, which had 27% drift between the means of the top and bottom row. The day 3 MTT assay also had a drift of 19%, just below the significance threshold of 20% [95]. Such plate effects, caused by experimental errors, increase CV values and thus decrease the value of Z'. However, as these effects were not consistent or predominant across multiple experiments, they can be considered insignificant to the overall investigation [95].

3.12 | Assessment of the suitability of 5GSH-6943#5 cells for high-throughput screening.

Once it was established that 5GSH-6943#5 cells responded well to androgen deprivation in the CSS condition, min-max signal variability assays were performed to determine whether this cell line would be suitable for high throughput screening using the assay developed in this project. Assays were performed comparing cell viability in FBS (maximum) against the androgen deprivation conditions of either CSS or FBS + 1 µM MDV (minimum). Data from

		MTT Assay						CellTiter-Blue					
		Day 3			Day 5			Day 3			Day 5		
Cell line	Exp.	CV FBS	CV FBS + MDV	Z'	CV FBS	CV FBS + MDV	Z'	CV FBS	CV FBS + MDV	Z'	CV FBS	CV FBS + MDV	Z'
CWR22PC_GB_22	1	7.74	13.93	0.09	3.41	10.26	0.74	10.02	13.44	-1.33	3.40	10.05	0.22
	2	6.25	12.10	0.15	9.62	16.10	0.40	5.21	6.95	-0.69	11.91	18.71	-0.48
CWR22PC_GB_06	1	21.92	26.52	-4.27	11.77	21.83	0.07						
		Confluence of MTT plate						Confluence of CellTiter-Blue plate					
		Day 3			Day 5			Day 3			Day 5		
Cell line	Exp.	CV FBS	CV FBS + MDV	Z'	CV FBS	CV FBS + MDV	Z'	CV FBS	CV FBS + MDV	Z'	CV FBS	CV FBS + MDV	Z'
CWR22PC_GB_22	1				5.50	8.78	0.59				8.89	21.82	0.30
	2	8.11	14.43	-0.72	10.79	13.15	0.22	14.32	16.26	-1.27	10.42	17.19	0.07
CWR22PC_GB_06	1	17.33	23.25	-2.83	15.55	13.73	-0.89						

Table 3: Summary of Coefficient of Variance (CV) and Z' data from min-max assays between FBS and FBS + MDV conditions in the CWR22PC_GB_22 cell line clone.

these experiments is summarised in table 4 and Figure 20. All plates were read using the MTT assay: experiments using CellTiter-Blue were not carried out based on min-max data in human cells (Figure 19, Table 3). As in CWR22PC cells, Z' values were highest at 5 days: at 3 days Z' values were all negative, indicative of an assay with very limited use in high-throughput screening [94]. Notably, there was little change in the effect size between day 3 and day 5 when comparing FBS to either FBS + MDV (Figure 20A) or to CSS (Figure 20B), however, the coefficients of variance were much lower at day 5, indicating more reproducible results. When comparing FBS and FBS + MDV, the Z' values were too low for high-throughput screening even at day 5. As the CV values at day 5 were low and indicative of good reproducibility between replicates, the lack of utility of this assay was mainly due to the small effect size between FBS and FBS + MDV (15-25%). The two Z' values in this experiment differed greatly due to a smaller effect size in the second repeat, possibly due to a seeding error leading to confluence being high enough for cells to begin to undergo contact inhibition by day 5. CSS had a much larger (50-60%) effect on total cell viability compared to FBS: again, the coefficients of variance were at an acceptable level, yet Z' values were only 0.16 and 0.24. Whilst these Z' scores are fairly low and have less ability to rank 'hits', they still have use for binary hit identification, and thus this assay would still be suitable as a base for a smaller-scale screen with an approved drug library. It should also be noted that we identified another stock of FBS which conferred a greater difference on 5GSH-6943#5 cell growth compared to androgen deprivation conditions than the FBS used in these experiments (Figure 10D): use of this or another serum would increase the effect of ADT, and would likely increase these Z' values.

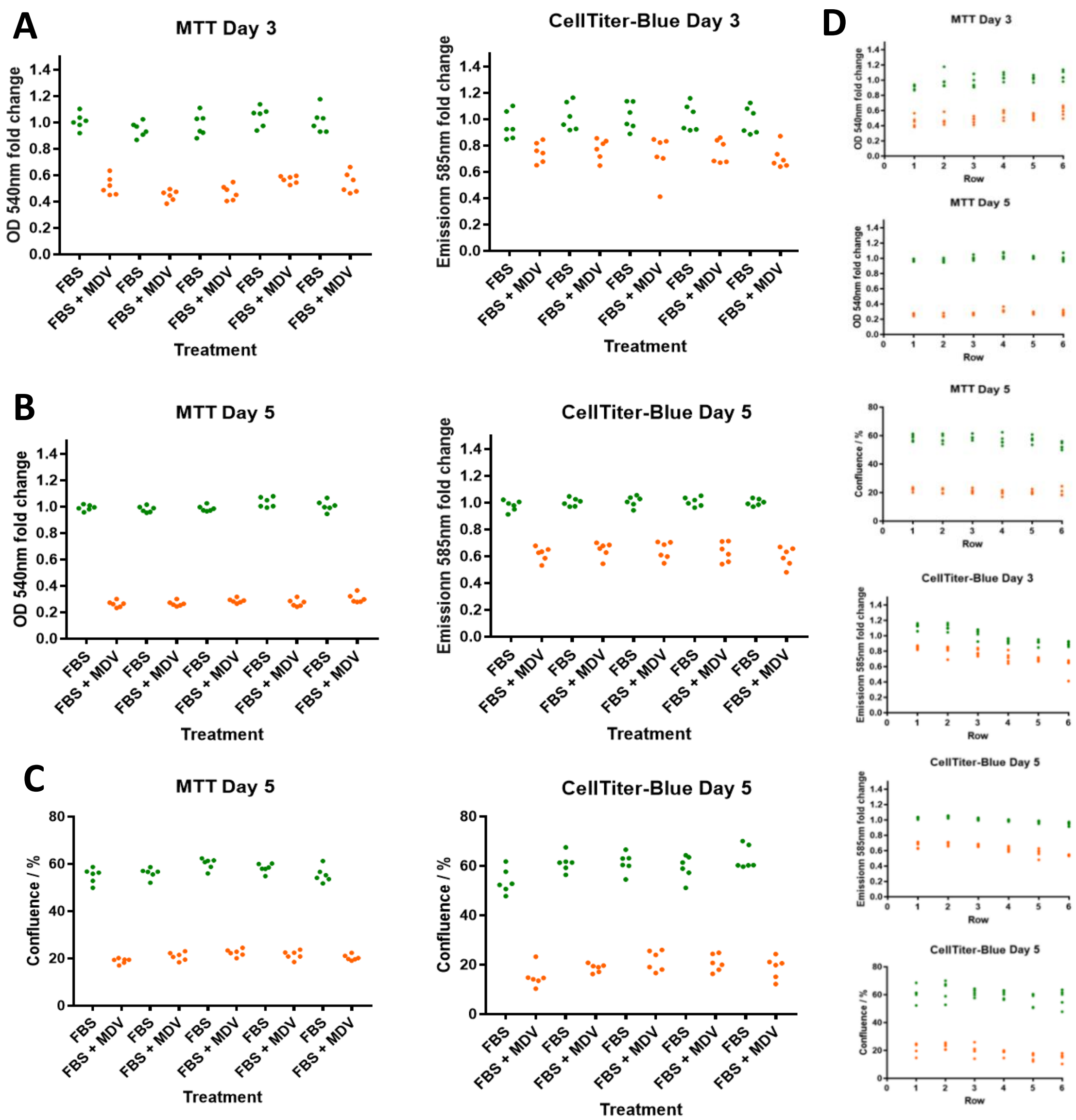

Figure 19: **Results of Min-Max assay in CWR22PC_GB_22 cells**. Scatter plot of single representative min-max assay between FBS and FBS + 1µM MDV conditions in the CWR22PC_GB_22 clone, seeded at 7000 cells/well 2 days before treatment. Data taken from min-max experiment 1 (Table 3). Measured by MTT assay and by CellTiter-Blue assay at 3 days **(A)** and 5 days **(B)**. **(C)** Confluence values of day 5 min-max assay plates assayed in (B) as measured with an IncuCyte Zoom® microscope, 4 images per well at 10X objective. Data for (A-C) organised per 6-well column, alternating between FBS (green) and FBS + 1µM MDV conditions. **(D)** Data from (A-C) transposed and presented by rows across the plate, 10 replicates per row. Wells in FBS displayed in green, in FBS + 1 µM MDV in orange.

		Day 3						Day 5					
Cell line	Exp.	CV FBS	CV FBS + MDV	Z'	CV FBS	CV CSS	Z'	CV FBS	CV FBS + MDV	Z'	CV FBS	CV CSS	Z'
5GSH-6943#5	1	8.65	12.26	-1.59	14.82	15.01	-0.43	3.83	5.46	0.07	10.92	8.78	0.16
	2	13.08	17.78	-2.64	10.29	17.88	-0.36	4.86	8.32	-1.63	7.95	8.65	0.24

Table 4: Summary of Z' and coefficient of variance (CV) values for min-max assays comparing FBS to either charcoal stripped serum (CSS) or administration 1 µM enzalutamide (MDV), in 5GSH-6943#5 cells (2 experiments, 500 cells/well seeded in 96 well plates, MTT assay at either 3 or 5 days). Each comparison a different plate.

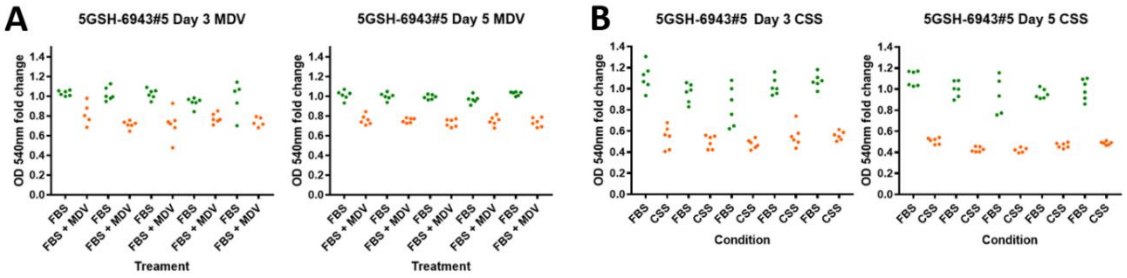

Figure 20: 5GSH-6943#5 androgen deprivation min-max experiments. Total viability of 5GSH-6943#5 cells at day 3 and day 5 of min/max assay, as measured by MTT assay. One representative experiment displayed (experiment 1 on Table 4). OD 540nm normalised to mean FBS value. 500 cells/ well seeded on 96 well plates. **(A)** Viability at day 3 and day 5 for min-max assays between FBS and FBS + 1μM MDV. **(B)** Viability at day 3 and day 5 for min-max assay between FBS and CSS.

Based on the response of the 5GSH-6943#5 cells to C3H10T1/2 cell conditioned media, min-max assays were also performed to establish whether the effect size of total cell viability between unconditioned and MSC-conditioned was sufficient for high-throughput screening. Assays at day 3 were not performed, due previous experiments showing high CV and low Z' values (Table 4). Assays compared FBS to FBS-CM and CSS to CSS-CM, with the data summarised in Table 5 and Figure 21. Confirming previous data (Figure 18), there was a sizable positive response to conditioned media in the CSS condition, but in the FBS condition CM had no effect. Despite this, high coefficients of variance and a relatively low effect size produced a negative Z' value between CSS and CSS-CM, indicating that this assay is not suitable for a HTS in its current form. CV values were markedly higher than those at day 5 in this cell line for androgen deprivation assays: the reasons for this are not clear. The proportional response to conditioned media was shown to be larger by measurement of confluence (Figure 21B) than by MTT assay (Figure 21A), in contrast to CWR22PC cells (Figure 19), however confluence readings also had much greater coefficients of variance, and so yielded even less suitable Z' values. The high CV values may be due to the characteristics of growth of 5GSH-6943#5 cells in the well: cells are seeded at very low density and grow into small clustered colonies rather than uniformly across the plate, or to collect at the edge of the well. These effects may confound the accurate association of the confluency metric with cell number and thus cell growth.

Z' values differed substantially between repeats using the same assay. This was likely due to inconsistency in the concentration of growth stimulating factors in the conditioned media, due to variation in the number of C3H10T1/2 cells present during CM production. Drift effects of 21% (in the MTT assay data) across the columns of the plate were also seen in the first experiment comparing CSS and CSS-CM, both (Figure 21A, left panel; Figure 21B, left panel), although these were not consistent between experiments.

		CSS / CSS-CM								FBS / FBS - CM							
		MTT Assay				Confluence				MTT Assay				Confluence			
Cell line	Exp.	Fold change	CV CSS	CV CSS-CM	Z'	Fold change	CV CSS	CV CSS-CM	Z'	Fold change	CV FBS	CV FBS-CM	Z'	Fold change	CV FBS	CV FBS-CM	Z'
5GSH-6943#5	1	1.57	14.58	8.36	-0.46	1.8	20.72	16.58	-0.90	0.96	7.77	8.61	-13.98	1.03	15.22	17.21	-31.20
	2					1.54	29.11	27.70	-2.95	0.97	7.98	11.03	-19.97	0.85	16.48	29.76	-7.50
	3	1.26	12.15	18.02	-2.84	1.59	36.53	25.84	-2.91								

Table 5: Summary of min-max assay Z', coefficient of variance (CV) and fold change (between normal and conditioned media) values for 5GSH-6943 cells, comparing control and C3H10T1/2 – cell conditioned medium with either 10% standard FBS or charcoal-stripped FBS (CSS). Assays performed over 5 days in a 96 well plate, data read by MTT (OD 540nm) or confluence.

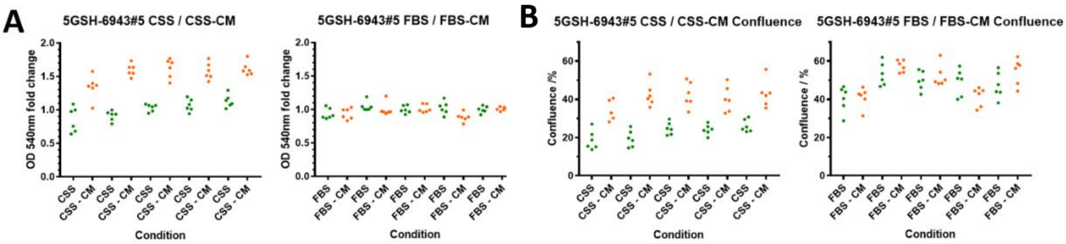

Figure 21: 5GSH-6943#5 conditioned media min-max experiments. Data for one representative experiment shown (experiment 1 on Table 5 for both conditions). **(A)** Total viability of 5GSH-6943#5 cells at day 5 of assay, as measured by MTT assay. OD 540nm normalised to mean CSS or FBS value. Means of 6 replicates in column, +/- S.E.M. **(B)** Confluence data, measured by IncuCyte Zoom® microscope, 4

Chapter 4 | Discussion

In this project, five clones of the androgen-sensitive human prostate cancer cell line CWR22PC were characterised for their response to androgen deprivation. A 96-well plate cell growth assay was then designed and optimised to test the response (by total cell viability) of some CWR22PC clones and murine 5GSH-6943#5 prostate cancer cells to MSC-conditioned media. Initial validation experiments were then performed on tested cell lines to assess the potential for use of the assay in a high-throughput screen. However, the ability of the assay to separate the two controls, as indicated by Z', was not indicative of an assay suitable for drug screening, due to an insufficient effect size of MSC-conditioned medium on prostate cancer cell growth.

Drug discovery through high throughput screening is an expensive process, and early go/no-go decisions are made based on primary screens using assays such as the subject of this project [101]. A screen is only as good as the assay on which it is based, and thus it is crucial that this assay sufficiently recapitulates the *in vivo* pathophysiological environment. At present, however, there are few drug discovery studies incorporating stromal cells, despite their relevance to anticancer therapy: in prostate cancer, multiple studies have indicated that MSCs stimulate tumour growth and resistance to androgen deprivation therapy [65,66,75]. However, such studies have not yet been performed using the CWR22PC prostate cancer cell line. The assay designed in this project is thus important both to characterise the effect of MSCs on CWR22PC cells during androgen deprivation and to provide a drug screening assay platform more relevant to the *in vivo* environment, to better identify potential effective treatments for CRPC.

4.1 | Implications and limitations of low throughput androgen deprivation assays

Initial experiments showed a strong response to androgen deprivation in all CWR22PC clones (Figure 7), whilst all bar the CWR22PC_GB_22 clone responded positively to additional DHT (Figure 8). However, the size of the response differed considerably between different clones, demonstrating heterogeneity in the CWR22PC cell line. Within tumours, clonal selection gives rise to heterogenous phenotypes [102]: progression to CRPC will thus occur in only a subpopulation of tumour cells *in vivo*, or by different mechanisms in different subpopulations. Notably, DHT produced a several-fold increase in viability in CSS in all clones, but this was only statistically significant for CWR22PC_GB_25. This is likely due to high variation in the raw optical density values (measuring the absorbance of the purple MTT product formazan) between the three experiments performed for each condition, particularly in CSS + DHT, giving large differences in the size of the response. This may be due to inconsistency in the number of cells seeded between repeat experiments: as growth was greatly increased by 1nM DHT compared to CSS alone, differences of a few hundred or thousand initial cells between experiments would be amplified to large differences in the effect size of DHT between these repeats. Additional repeats of this experiment would possibly reveal statistical significance of these results, otherwise an alternative approach, for example using a different method of cell counting or to ensure more equal cell seeding between different experiments, may have yielded more consistent results.

Some clones also gave negative OD readings once DMSO background was subtracted, despite the presence of cells upon microscopic inspection. This may be due to insufficient sensitivity of the MTT assay in detecting low cell numbers. In addition, washing cells with PBS, adding DMSO to solubilise formazan and transferring formazan solution to a 96 well plate after MTT incubation may have introduced errors reducing the OD signal below background controls, and may have increased the variation between replicate wells. Optimising seeding density, MTT incubation time and the concentration of MTT added may improve the sensitivity of the assay.

4.2 | Use of charcoal-stripped serum as a means of androgen deprivation

CSS produced a stronger negative effect on growth compared to FBS than enzalutamide (MDV) in all CWR22PC clones, whilst in three of the clones FBS + DHT gave a higher signal than CSS + DHT. In addition to androgens, other steroid hormones, thyroid hormones and even some peptide hormones (such as alkaline phosphatase, lactate dehydrogenase and aspartate aminotransferase)., as well as glucose, vitamins such as folic acid and vitamin B12, and electrolytes such as magnesium, phosphorus, calcium and potassium have been shown to be reduced in charcoal stripping of FBS [103]. The use of CSS as a model of androgen deprivation is therefore not entirely comparable to growth in FBS or as relevant to the environment *in vivo* during ADT, as some of the reduced effect on growth compared to FBS may be due to the depletion of these other factors. Notably, however, this effect was not seen in all clones. CSS can instead be compared to CSS + DHT, although a 1nM dose of DHT produced a much higher response than FBS alone in these experiments, and large differences were found between the CSS + DHT + MDV and FBS + MDV conditions in three of the clones (Figure 9). Inclusion of an FBS + DHT condition may provide further insight into the DHT response of prostate cancer cells, and into differences between FBS and CSS through comparison with CSS + DHT.

4.3 | Androgen responsiveness in the 5GSH-6943#5 cell line

Experiments using the murine prostate cancer cell line 5GSH-6943#5 required significant troubleshooting due to the lack of response to androgen deprivation of cells initially used, to ascertain whether the unexpected results were due to a fault with reagents and to investigate the unexpected response to DHT (Figure 10A). When a different batch of 5GSH-6943#5 cells was used, this cell line was found to respond to androgen deprivation and additional DHT as expected, but showed a smaller response to ADT than CWR22PC cells (Figure 10D). Notably the Myc-CaP cell line (from 5GSH-6943#5 cells are derived) possesses greatly elevated AR expression [86] which may explain the reduced castration sensitivity of 5GSH-6943#5 cells in comparison to CWR22PC [16]. However, Watson et al reported a 6.2-fold higher colony formation in FBS compared to CSS in the Myc-CaP cell line from which 5GSH-6943#5 is derived: the lower CSS response in 5GSH-6943#5 cells indicated in our experiments may be due to clonal heterogeneity in the Myc-CaP cell line. Secondly, CSS had a much larger effect than 1 µM enzalutamide: a possible explanation for this is difference between the AR in human and murine cell lines reducing the ability of enzalutamide to inhibit the receptor. Whilst the ligand-binding and DNA-binding domains of human and murine AR are identical, there is only 76% similarity in the *N*-terminal regulatory domain [104]. AR is amplified in this cell line (Watson), possibly reducing the effectiveness of enzalutamide inhibition. Furthermore, the removal of non-androgenic compounds during charcoal treatment of serum may comprise a large amount of this difference: notably, CSS + 1nM DHT gave a considerably lower signal than FBS alone. However, other studies have shown found that 1nM of the synthetic androgen R1881 in CSS completely rescued Myc-CaP growth compared to FBS [86].

4.4 | Collection of confluence data over time using the IncuCyte Zoom®

Experiments to find optimum seeding density for 96-well plate experiments were conducted over 5 days to avoid excessive nutrient depletion, thus extrapolation for an additional day was required to estimate the optimum cell density. Accurate estimation was difficult in 5GSH-6943#5 cells due to their high growth rate, leading to initial experiments using excessive seeding densities and requiring assaying on day four to avoid overconfluence. Low initial seeding density increased the proportional effect of approximations inherent in the (automated) cell counting, which were then amplified by high growth rate to give a high level of variation in final cell number between repeat experiments. Performing cell density experiments over six rather than five days, changing media 24 hours after seeding, as in other experiments, may have improved estimation of the correct cell density.

In contrast to 5GSH-6943#5 cells, CWR22PC cells grew very slowly, such that, except for the CWR22PC_GB_22 clone (Figure 11D), the confluence traces do not appear to show cells growing in the logarithmic phase. This complicated estimation of the optimal seeding density for these clones. Also, the CWR22PC_GB_02 and 06 traces (Figures 11A, B) show fluctuations in recorded confluence, likely caused by opening and closing of the drawer of the IncuCyte Zoom® to add and remove plates, leading to shifts in the camera position between readings. In a few cases, these shifts could cause the microscope to take images including the edge of the well or beyond introducing considerable error. Use of ImageLock plates, which possess a marker tracked by the IncuCyte Zoom® ensuring image capture of the same well area each time, would have prevented these errors.

4.5 | The effect size of MSC-conditioned media was insufficient for HTS and requires further optimisation

Experiments using MSC-conditioned media in human cells produced only a modest effect. Whilst CWR22PC_GB_22 responded positively to conditioned media, the effect size was small and not statistically significant (Figure 14A). Although cell line availability issues meant that min-max experiments assessing the effect of CM in CWR22PC cells were not performed, Z’ values obtained using the 5GSH-6943#5 cell line, which had a greater response to CM, suggest that the effect would likely not be large enough to produce a sufficient Z’ value. Administration of fresh conditioned media after 3 days would likely increase effect size in the cell line, as it did (albeit modestly) in 5GSH-6943#5 cells (Figure 17). Reuse of CM used on day 0 at day 3 had no additional effect compared to not changing media (Figure 16), indicating that the factor(s) responsible for stimulating growth is or are inactivated after 72 hours at 4ºC. For all experiments conditioned media was diluted 1:2 into regular media to mitigate depletion of growth factors and nutrients by the MSCs. A higher proportion of conditioned media may have a greater effect on growth, although the greater depletion of nutrients and growth factors may lead to the opposite effect. This may be optimised by investigation of different dilution ratios.

In preliminary experiments the CWR22PC_GB_02 and 06 clones had a stronger response to MSC-conditioned medium than CWR22PC_GB_22 cells (Figure 14A, B, C). These clones, CWR22PC_GB_06 in particular, may therefore be better candidates for high throughput screening, though both grew at a lower rate than CWR22_GB_22. One-way analysis of variance (ANOVA) on a single experiment for each clone showed a significant response to conditioned media for both clones, however as these results are only from a single experiment this analysis is of limited validity, as asserting statistical significance requires at least three biological replicates. Repeat experiments could not be performed in these clones due to mycoplasma infection of primary BM-MSCs. As they would not tolerate cryopreservation, the cells could not be replaced. In addition, both CWR22PC cells and primary BM-MSCs grew very slowly, making it challenging to co-ordinate cell seeding and collection of conditioned media to perform multiple experiments efficiently.

The response to conditioned media was greatest in the FBS + 1µM enzalutamide condition for all CWR22PC clones tested: this is consistent with the *in vitro* results of Cheng *et al*. (2016) showing that MSC conditioned media completely rescued the growth of LNCaP cells grown in CSS and did not affect the growth of cells grown in the presence of androgen [75]. However, the CM response in our experiments was not nearly as great as Cheng et al: this may reflect differences between the CWR22PC and LNCaP cell lines. However, in our experiments the FBS + MDV - CM condition used conditioned media containing FBS: Cheng *et al*. found that the effect of conditioned media depended on MSCs also being deprived of androgen [75]. Future experiments could include enzalutamide in production of CM, or use CSS-CM added to FBS, to investigate whether depriving MSCs of androgen increases their effect on CWR22PC cells. This would also be more representative of *in vivo* pathophysiology, where both tumour and stromal cells undergo androgen deprivation. However, in this project the primary MSCs used did not survive after conditioning with media containing CSS, and thus FBS-CM was used for all conditions due to scarcity of MSCs. The serum used in the CSS condition is thus 1/3 FBS, and thus is not very representative of ADT *in vivo*. This presence of FBS in the CSS condition may limit the effect of CM, due to inhibition of MSC TGFβ production by androgen and by reducing the effect of ADT for MSC stimulation of castration resistance to rescue. However, CM did stimulate growth in the FBS condition in this cell line, particularly in CWR22PC_GB_06 cells, suggesting that the effects of MSCs on this cell line are unlikely to be solely due to stimulation of castration resistance and may involve multiple mechanisms. However, it is possible that MSC CM may increase response to the relatively low androgen concentration in FBS: supporting this, conditioned media in CSS + DHT, with higher levels of androgen, did not stimulate cell proliferation.

The response to murine MSC-conditioned media in 5GSH-6943#5 cells was broadly in line with CWR22PC cells. The increase in cell proliferation was greatest in the CSS condition (Figure 17), supporting the hypothesis that MSCs stimulate castration-resistant tumour growth. Unlike the primary human MSCs, the C3H10T1/2 MSCs used tolerated culture in CSS-containing media, allowing use of CSS-CM. In this sense results in this cell line are more representative of the *in vivo* condition than the CWR22PC experiments. C3H10T1/2 CM had a greater effect in the CSS condition than in FBS + MDV (which used FBS-CM), which may be due to ADT stimulating the effect of MSCs on castration-resistant growth. However, this may instead be due to the limited effect of 1 µM enzalutamide on 5GSH-6943#5 cells: if CM stimulates castration-resistant growth, its effect may be smaller if the growth inhibition of androgen deprivation is relatively slight. Repeating this experiment with higher doses of enzalutamide would help to ascertain if this is the case, but 1 µM is considered the clinically relevant dose of enzalutamide *in vivo* [15,45]. One could also further investigate the effect of androgen on CM effect by including enzalutamide in conditioned media for the FBS + MDV – CM condition, or by adding FBS-CM to the CSS condition and vice versa (although this would not replicate *in vivo* pathophysiology).

An inherent limitation of assays using conditioned media is reproducibility: it is difficult to estimate the number of MSCs present in the flask when media is changed and to keep this the same between experiments. Additional limitations in this project exacerbated this issue: CWR22PC cells required seeding a day before changing of MSC media, necessitating anticipation of when MSCs would at a suitable confluence. By contrast, C3H10T1/2 cells grew very quickly, thus media was changed when confluence was fairly low, requiring estimation of confluence 24 hours later. Care was needed to assure a maximal number of cells to secrete castration resistance-stimulating factors, without cells becoming over-confluent: C3H10T1/2 cells are highly sensitive to contact inhibition [87]. These effects led to a large degree of variation between repeat experiments, reducing the reliability of Z' scores as a measure of assay quality, and would undermine drug screening if repeated over multiple cell passages.

4.6 | Viability assays

Experiments using conditioned media utilised both CellTiter-Blue and MTT assays to measure total cell viability per well, to assess cellular proliferation. CellTiter-Blue has shown to be more sensitive to small changes and lower cell numbers than MTT [105], and is less prone to error [97], and thus would be expected to be the preferable assay. In our experiments, however, CellTiter-Blue showed much smaller differences between conditions than MTT (Figure 14D), thus giving substantially lower Z' values (Table 3). Additionally, despite CellTiter-Blue being read directly from the plate without having to wash wells and solubilise with DMSO, which one would expect to reduce error, coefficient of variance (CV) between replicates was no lower than with the MTT assay.

The reasons for the lower sensitivity of CellTiter-Blue in our investigations was not clear. It is possible that the three-hour incubation period with the assay reagent was too long, (something not revealed by a single optimisation experiment), or that cell number may have been too high for the assay to function effectively. If so, high rates of reduction by highly viable cells of high numbers of cells may have caused further reduction of the fluorescent product resorufin to the nonfluorescent hydroresorufin [93], reducing the signal in the well, whereas this will not occur as much in lower viability wells. This would lead to underestimation of cell number in high viability wells and a reduction in the apparent effect size. Further optimisation experiments, for example changing the concentration and incubation time of CellTiter-Blue, or applying it to a serial dilution of cells to determine the linear dynamic range, may have revealed these reasons and improved sensitivity.

Quantification of confluence is highly flawed as a measure of cell number. The density at which cells clustered together varies considerably and tended to increase with increasing confluence (Figure 10B). This would likely have caused underestimation of cell number at high confluence and overestimation at lower densities. The software used may also include as confluence spaces between cells that are close together but not in contact and dead or minimally viable cells that are not counted by viability assays, in addition to inorganic contaminants (such as fibres) background signal, particularly in cell lines which contrast poorly with the well surface. Accurate measurement of confluence also depends on cells being evenly spaced, yet cells tended to collect at the edge of wells outside the field of the micrograph, whilst 5GSH-6943#5 cells tended to grow into tight clusters.

In 24 well plate experiments, MTT solution was added directly to the culture medium already present in the well, as per the existing lab protocol. Lower pH in wells with higher cell density may have had confounding effects: at low PH values the absorbance peak of formazan is lower, broader and shifted to lower wavelengths [106]. In addition, the different growth conditions the cells were cultured in could affect the metabolic rate, and thus the level of MTT reduction by each cell. As previously discussed, there was a substantial amount of variation between replicates, and negative OD values at low viabilities. Use of a different assay would remove the need for washing or addition of DMSO, possibly removing sources of error and improving the consistency results. A resazurin reduction assay would be an obvious option, yet in this project sensitivity CellTiter-Blue was found to be substantially less sensitive, (though it was not tested on 24 well plates at a lower seeding density). Other formazan assays to MTT, such as XTT, WST-1 and CCK-8 have a higher sensitivity and form soluble formazans [107], removing the need for solubilisation with DMSO. Otherwise, assays measuring ATP concentration, such as CellTiter-Glo (Promega) may be preferable: CellTiterGlo is read by luminescence and thus does not require additional steps after addition of the assay reagent, has been shown to have considerably greater sensitivity than tetrazolium based assays, and is faster and simpler to use [108].

In contrast to low throughput experiments, MTT and CellTiter-Blue were added to 96-well plates by mixing in DMEM + 10% FBS and added after aspiration of the treatment media. This ensured an equal concentration of assay reagent between wells of the plate: if only 5 or 10 µL per well of reagent is added directly, pipetting errors of only a fraction of a microlitre will cause large errors in the reading. In addition, pH and media constituents were equal between wells using this method: these variables thus would not have confounding effects on the reduction rate. Incubating all cells in the same media over the reagent incubation period may help equalise the metabolic activity per cell between different groups, making the assay more representative of cell number per well, although cells may take longer to adjust to the change in condition than the brief incubation time. Conversely, changing the media to add the assay reagent may have caused loss of cells, which may be more likely in the ADT conditions which reduce cell viability, possibly leading to overestimation of the effect of androgen deprivation.

4.7 | High throughput screening: further optimisation required

Min-max assays using CWR22PC_GB_22 cells show low variance between replicates and a high Z’ between FBS and FBS + MDV conditions, indicating the design and execution of the assay is of acceptable quality (Figure 19, Table 3). However, a drug screen needs to include conditioned media to be informative, to identify compounds which inhibit MSC stimulation of castration-resistant growth. Considering the small effect size of MSC-CM in the CWR22PC_GB_22 clone (Figure 14A), it is unlikely that a min-max assay between normal and conditioned media in the FBS + MDV condition would yield a sufficient Z’ value. Min-Max assays between FBS and an androgen deprivation condition still help validate the protocol used, ensure that there are no errors such as drift effects, and judge whether the size of the ADT response is sufficient for drugs inhibiting MSC effects to be useful. Such an assay could also be used for screening compounds that may affect androgen sensitivity.

It is possible that further optimisation could increase the effect size of conditioned media and thus improve Z’ to a level where drug screening would be justified. This may involve changes to the protocol to obtain and use MSC-conditioned media, use of a different viability assay or use of different cell lines or clones. In this study, we showed that a media change at day 3 using fresh CM increased effect size in 5GSH-6943#5 cells (Figure 17), however the size of this increase was not enough to justify performing min-max experiments employing this media change, as doing so would be unlikely to raise Z’ sufficiently. Changing the media midway through an assay would likely cause cells to become stressed or lost, and may cause the concentration of compounds between wells to differ: this may increase the coefficient of variance and thus in fact reduce Z’. The process of changing the media also disturbs the conditions of the assay, reducing control over the environment and increasing variation between different plates.

The assay may also be improved by use of different cell lines which exhibit a stronger response to conditioned media. Cheng *et al.* (2016) show a strong response to MSC-CM in the LNCaP cell line [75], however LNCaPs are less androgen-sensitive than CWR22PC cells [31] and therefore may be a less suitable cell line for investigation of response to androgen deprivation therapy. The relatively low response of 5GSH-6943#5 cells to ADT may have limited the effect of MSCs on proliferation if MSCs function to stimulate castration resistance: identification of a more androgen sensitive cell line may allow for an increased effect of MSC CM. Identification of an alternative drug to enzalutamide may also give a larger ADT effect: this could be investigated through a pilot screen using a small, focused library of antiandrogens to identify the drug with the largest effect on a given cell line. However, enzalutamide is currently the drug given to patients when other forms of ADT has failed [24], and is thus likely the most relevant drug to include in a screen looking to identify new agents which could further increase the period of remission with ADT. Adding replicates to an assay for screening would also increase the power of the assay, although this would reduce the assay throughput [95].

There are flaws with the use of Z' to judge suitability for high throughput screening. Z' is a highly conservative measure of separation between positive and negative controls: at a Z' of 0.5, indicative of an 'ideal' assay [94], a full twelve standard deviations separate the two means. When Z'=0, commonly considered a 'useless' assay, the two means still differ by six standard deviations, and consequently there is less than a 1 in 90,000 chance of a positive response being less than a randomly chosen negative control value [109]. This would suggest that, particularly if the aim of a screen is merely to identify rather than rank hits, assays with Z' values considerably lower than 0.5 may still be useful for drug screening. High throughput screening is an expensive process and thus decisions on assay suitability will depend on weighing cost against the probability of success: a smaller, more targeted drug library may be suitable for assays with a Z' closer to zero. There are other problems with the use of Z' for a measure of assay quality: it is most often reported without confidence intervals (although CIs can be calculated), is biased, and lacks strong statistical underpinning [109].

4.8 | High throughput screening based on an optimised assay

Translation of this assay into a high throughput screen would require additional validation than min-max plate uniformity assessment assays to ensure that the assay is reproducible. As detailed by Iversen *et al.*, this would require testing 20-30 compounds in the assay over two runs, and the results compared to measure reproducibility and variation in the potencies of these compounds between runs. There must be sufficiently little within-run and between-run variability for screening to go ahead [95]. Notably, automation of processes in a high throughput screen would likely decrease coefficient of variance and improve Z' value.

Once an appropriately optimised assay has been shown by assay validation to be reproducible and to possess a sufficient assay window for hit detection, a screen would likely test an approved drug library to repurpose existing drugs, or a small library of diverse chemical structures to develop novel drugs, at either a single concentration or across a small range of concentrations (for example, 1, 5 and 10 µM). Success of drug screening depends not just on the quality of the assay on which it is based but on the drug library used. Library quality depends on a both inclusion of many widely diverse compounds and a focus on those with drug-like properties which are likely to have some activity on the target molecule or cell phenotype and thus produce screening hits. Optimisation of a screen must balance maximising the probability of identification of hit compounds and the time and monetary costs of performing the screen, which will increase with the size of the library [96].

Drugs detected as a 'hit' can then be studied further in more detailed dose-response experiments, using at least five different concentrations, to better characterise their effects on castration-resistant prostate cancer cell growth and calculate the EC50 for that compound. EC50 gives a measure of the potency of the compound, allowing the most promising hits to be identified. Hits with sufficient potency can then be further investigated, for example by studying their chemical structure to inform design of novel lead compounds by other more targeted drug discovery programs. Leads are unlikely to be identified directly from a screen, but usually require further assays on similar compounds to further optimise the candidate compound [96]. Investigation of the mechanism of action of hit compounds in promoting castration may also be performed, for example by analysis of their chemical structure or by using comparative phenotypic screening techniques such as theta cell comparative scoring [99].

4.9 | Future directions

The chance of lead compounds being developed from screening hits depends not only on the size and relevance of the drug library used, but also on an assay closely enough representing the *in vivo* environment and disease pathophysiology. Future experiments, therefore, should utilise direct coculture of MSCs and cancer cells. A direct coculture assay would include the effects of cell-cell contact between MSCs and cancer cells, and of crosstalk between the two cell types, as MSC phenotypes are affected by signalling from tumour cells [53,69]. In such an assay MSCs and cancer cells would both be exposed to the same conditions: as shown by Cheng *et al.*, the level of androgen deprivation appears to be of importance in the effect of MSCs [75]. Such a study was beyond the scope of this project, however, as the IncuCyte Zoom® was unable to distinguish between MSCs and prostate cancer cells and thus proliferation of prostate cancer cells alone could not be quantified. This investigation would require fluorescent cell labelling of distinct cell types, to enable detection of changes in prostate cancer cell number alone. Such a study would also require optimisation of seeding of both MSCs and prostate cancer cells in the same well, and may make comparison with cancer cell growth in the absence of MSCs more difficult. Relevance to the environment *in vivo* also depends on how closely the cell lines used represent the phenotypes of prostate cancer cells and MSCs in the tumour. Whilst experiments in human cells utilised primary bone marrow MSCs, experiments in murine cells used the MSC cell line C3H10T1/2: whilst BM-MSCs are a heterogenous population, C3H10T1/2 cells are homogenous and this cannot replicate the variety of phenotypes found *in vivo* [90].

The assay format could be further elaborated upon to increase relevance to disease pathophysiology. Coculture of MSCs and tumour cells still does not include the complex network of interactions and signalling between tumour cells and many types of stromal and immune cells forming the tumour niche [53]. One could attempt to better represent the tumour microenvironment by designing a coculture assay using more than two cell populations, although this will increase the complexity of optimising the assay. Restriction of cell culture to a two-dimensional cell surface also limits relevance to disease pathophysiology, as a cell monolayer cannot replicate the structure and spatial organisation of the tumour microenvironment [110]; in addition, drug kinetics may differ and 2D experiments give have effective doses which are not effective when scaled to patients [101].

Recent developments have been made in design of three-dimensional organoid tumour models using extracellular matrix (for example Matrigel) frameworks [110]. These most commonly only include a single cell population; however, hybrid organoids have been constructed using multiple cell types. For example, to investigate liver metastasis, Skardal et al (2015) created organoids including both hepatoma and colon carcinoma cells using simulated microgravity bioreactors, allowing cells to recapitulate the three-dimensional organisation present *in vivo*. Cancer cells cultured in the organoid structures possessed a notably different phenotype indicative of epithelial-mesenchymal transition (EMT), more in line with the metastasis-associated cell phenotype *in vivo* [101]. Organoid cancer models have also been used in a 384-well format for high throughput screening by Boehnke *et al.* (2016): assay validation gave low CV values and high Z' values above 0.5 [111]. However, there may be added complexity in HTS with hybrid organoids in assessment of cell proliferation. The extracellular matrix (ECM) may also play a role in cell behaviour relevant to the pathophysiology of cancer: both two- and three-dimensional tissue matrix arrays can be used in high throughput screening to include cell-ECM interactions. These arrays were created by chemical treatment of harvested porcine tissue to remove cellular material, before lysophiling into nanoparticles that retained the structure and proteomic complexity of ECM *in vivo* [112]. The 3D microarrays were compatible with metabolic assays, and may further improve the relevance of HTS and thus the likelihood of lead compounds being effective *in vivo*.

4.10 | Conclusion

This project has thus demonstrated a positive effect of mesenchymal stem cell conditioned media on the growth of both human and murine prostate cancer cells, particularly under the condition of androgen deprivation. This supports the hypothesis that MSCs of the tumour stroma support acquisition of resistance of the tumour to androgen deprivation therapy. However, assay validation experiments show that further optimisation is required for this assay to be used to screen a drug library for compounds that could inhibit this effect. Such compounds, if investigated further, could be developed into lead compounds for development of drugs to prolong remission of prostate cancer.

References

1. Siegel R, Naishadham D, Jemal A. Cancer Statistics, 2013. *CA Cancer J Clin*. 2013;63(1):11-30. doi:10.3322/caac.21166.

2. Cancer Research UK. Prostate Cancer Statistics. http://www.cancerresearchuk.org/health-professional/cancer-statistics/statistics-by-cancer-type/prostate-cancer#heading-Zero. Published 2017. Accessed September 2017.

3. Harris WP, Mostaghel E, Nelson PS, Montgomery B. Androgen deprivation therapy: progress in understanding mechanisms of resistance and optimizing androgen depletion. *Nat Clin Pr Urol*. 2009;6(2):76-85. doi:10.1038/ncpuro1296.Androgen.

4. Bubendorf L, Schöpfer A, Wagner U, *et al.* Metastatic patterns of prostate cancer: An autopsy study of 1,589 patients. *Hum Pathol*. 2000;31(5):578-583. doi:10.1053/hp.2000.6698.

5. Cooperberg MR, Hinotsu S, Namiki M, *et al.* Risk assessment among prostate cancer patients receiving primary androgen deprivation therapy. *J Clin Oncol*. 2009;27(26):4306-4313. doi:10.1200/JCO.2008.21.5228.

6. Shiota M, Itsumi M, Takeuchi A, *et al.* Crosstalk between epithelial-mesenchymal transition and castration resistance mediated by Twist1/AR signaling in prostate cancer. *Endocr Relat Cancer*. 2015;22(6):889-900. doi:10.1530/ERC-15-0225.

7. Sharifi N, Gulley JL, Dahut WL. An Update on Androgen Deprivation Therapy for Prostate Cancer. *Endocr Relat Cancer*. 2010;17(4):R305-R315. doi:10.1007/s12020-009-9266-z.A.

8. Gralow JR, Biermann JS, Farooki A, *et al.* NCCN Task Force Report: Bone Health in Cancer Care. *J Natl Compr Canc Netw*. 2013;11(Suppl 3):S1-32. http://www.pubmedcentral.nih.gov/articlerender.fcgi?artid=3047404&tool=pmcentrez&rendertype=abstract.

9. National Institute for Health and Care Excellence (NICE). *Prostate Cancer: Diagnosis and Management. Clinical Guideline [CG175]*. https://www.nice.org.uk/guidance/CG175. Accessed September 1, 2017.

10. Huggins, C; Stevens, R.E.; Hodges C. Studies On Prostatic Cancer: II. The Effects Of Castration On Advanced Carcinoma Of The Prostate Gland. *Arch Surg*. 1941;43(2):209-223.

11. Wong YNS, Ferraldeschi R, Attard G, de Bono J. Evolution of androgen receptor targeted therapy for advanced prostate cancer. *Nat Rev Clin Oncol*. 2014;11(6):365-376. doi:10.1038/nrclinonc.2014.72.

12. Seidenfeld J, Samson D, Hasselbad V, *et al.* Single-Therapy Androgen Suppression in Men with Advanced Prostate Cancer: A Systemic Review and Meta-Analysis. *Ann Intern Med*. 2000;132:566-577. doi:10.7326/0003-4819-132-7-200004040-00009.

13. van Poppel H, Nilsson S. Testosterone Surge: Rationale for Gonadotropin-Releasing Hormone Blockers? *Urology*. 2008;71(6):1001-1006. doi:10.1016/j.urology.2007.12.070.

14. Taplin M-E, Rajeshkumar B, Halabi S, *et al.* Androgen Receptor Mutations in Androgen-Independent Prostate Cancer: Cancer and Leukemia Group B Study 9663. *J Clin Oncol*. 2003;21(14):2673-2678. doi:10.1200/JCO.2003.11.102.

15. Tran C, Ouk S, Clegg NJ, *et al.* Development of a Second-Generation Antiandrogen for Treatment of Advanced Prostate Cancer. *Science (80-)*. 2009;324(5928):787-790. doi:10.1126/science.1168175.Development.

16. Chen CD, Welsbie DS, Tran C, *et al.* Molecular determinants of resistance to antiandrogen therapy. *Nat Med*. 2004;10(1):33-39. doi:10.1038/nm972.

17. Balbas MD, Evans MJ, Hosfield DJ, *et al.* Overcoming mutation-based resistance to antiandrogens with rational drug design. *Elife*. 2013;2013(2):1-21. doi:10.7554/eLife.00499.

18. Scher HI, Fizazi K, Saad F, *et al.* Increased survival with enzalutamide in prostate cancer after chemotherapy. *N Engl J Med*. 2012;367(13):1187-1197. doi:10.1056/NEJMoa1207506.

19. Scher HI, Anand A, Rathkopf D, *et al.* Antitumour activity of MDV3100 in castration-resistant prostate cancer: A phase 1-2 study. *Lancet*. 2010;375(9724):1437-1446. doi:10.1016/S0140-6736(10)60172-9.

20. NCIN. *Major Resections by Routes to Diagnosis (2006 to 2010; England)*. London; 2015. http://www.ncin.org.uk/publications/reports/. Accessed September 2017

21. Lu-Yao GL, Albertsen PC, Moore DF, *et al.* Survival Following Primary Androgen Deprivation Therapy Among Men With Localized Prostate Cancer. *JAMA*. 2008;300(2):173. doi:10.1001/jama.300.2.173.

22. National Institute for Health and Care Excellence (NICE). Prostate Cancer: Treatment Summary. BNF. https://bnf.nice.org.uk/treatment-summary/prostate-cancer.html. Published 2017. Accessed September 1, 2017.

23. National Institute for Health and Care Excellence (NICE). *Degarelix for Treating Advanced Hormone-Dependent Prostate Cancer - Guidance [TA404].*; 2016. https://www.nice.org.uk/guidance/ta404/resources/degarelix-for-treating-advanced-hormonedependent-prostate-cancer-pdf-82604542759621. Accessed September 2017

24. National Institute for Health and Care Excellence (NICE). *Enzalutamide for Metastatic Hormone-relapsed Prostate Cancer Previously Treated with a Docetaxel-containing Regimen - Guidance [TA316]*. London; 2014. https://www.nice.org.uk/guidance/ta316. Accessed September 2017

25. Lin T, Izumi K, Lee SO, Lin W, Yeh S, Chang C. Anti-androgen receptor ASC-J9 versus anti-androgens MDV3100 (Enzalutamide) or Casodex (Bicalutamide) leads to opposite effects on prostate cancer metastasis via differential modulation of macrophage infiltration and STAT3-CCL2 signaling. *Cell Death Dis*. 2013;4(8):764-769. doi:10.1038/cddis.2013.270.

26. Wilderer P. Bioassays for Estrogenic and Androgenic Effects of Water Constituents. In: Wilderer P, Rogers P, Uhlenbrook S, Frimmel F, Hanaki K, Vereijken T, eds. *Treatise on Water Science, Volume 3*. Newnes; 2010:1805.

27. Debes JD, Tindall DJ. Mechanisms of Androgen-Refractory Prostate Cancer. *N Engl J Med*. 2004;351(15):1488-1490. doi:10.1056/NEJMp048178.

28. Heinlein CA, Chang C. Androgen receptor in prostate cancer. *Endocr Rev*. 2004;25(2):276-308. doi:10.1210/er.2002-0032.

29. Takahashi S, Watanabe T, Okada M, *et al.* Noncanonical Wnt signaling mediates androgen-dependent tumor growth in a mouse model of prostate cancer. *Proc Natl Acad Sci*. 2011;108(12):4938-4943. doi:10.1073/pnas.1014850108.

30. Tan J-A, Sharief Y, Hamil KG, *et al.* Dehydroepiandrosterone activates mutant androgen receptors expressed in the androgen-dependent human prostate cancer xenograft CWR22 and LNCaP cells. *Mol Endocrinol*. 1997;11(4):450-459. doi:10.1210/mend.11.4.9906.

31. Dagvadorj A, Tan SH, Liao Z, Cavalli LR, Haddad BR, Nevalainen MT. Androgen-regulated and highly tumorigenic human prostate cancer cell line established from a transplantable primary CWR22 tumor. *Clin Cancer Res*. 2008;14(19):6062-6072. doi:10.1158/1078-0432.CCR-08-0979.

32. Tepper CG, Boucher DL, Ryan PE, *et al.* Characterization of a novel androgen receptor mutation in a relapsed CWR22 prostate cancer xenograft and cell line. *Cancer Res*. 2002;62(22):6606-6614.

33. Robinson D, Van Allen EM, Wu Y-M, Schultz N, Sawyers CL, Chinnaiyan AM. Inegrative clinical genomics of advanced prostate cancer. *Cell*. 2015;161(5):1215-1228. doi:10.1038/nature15540.Genetic.

34. Zhu M-L, Kyprianou N. Androgen receptor and growth factor signaling cross-talk in prostate cancer cells. *Endocr Relat Cancer*. 2008;15(4):841-849. doi:10.1677/ERC-08-0084.

35. Marques RB, Dits NF, Erkens-Schulze S, van Weerden WM, Jenster G. Bypass mechanisms of the androgen receptor pathway in therapy-resistant prostate cancer cell models. *PLoS One*. 2010;5(10):e13500. doi:10.1371/journal.pone.0013500.

36. Chen Y, Sawyers CL, Scher HI. Targeting the androgen receptor pathway in prostate cancer. *Curr Opin Pharmacol*. 2008;8(4):440-448. doi:10.1016/j.coph.2008.07.005.Targeting.

37. Linja MJ, Savinainen KJ, Sarama OR, Tammela TLJ, Vessella RL, Visakorpi T. Advances in Brief Amplification and Overexpression of Androgen Receptor Gene in Hormone-Refractory Prostate Cancer 1. *Cancer Res*. 2001;61:3550-3555.

38. Visakorpi T, Hyytinen E, Koivisto P, *et al.* In vivo amplification of the androgen receptor gene and progression of human prostate cancer. *Nat Genet*. 1995;9(4):401-406. doi:10.1038/ng0495-401.

39. Li R, Wheeler T, Dai H, Frolov A, Thompson T, Ayala G. High level of androgen receptor is associated with aggressive clinicopathologic features and decreased biochemical recurrence-free survival in prostate: cancer patients treated with radical prostatectomy. *Am J Surg Pathol*. 2004;28(7):928-934. http://www.ncbi.nlm.nih.gov/pubmed/15223964.

40. Niu Y, Altuwaijri S, Lai KP, *et al.* Androgen receptor is a tumor suppressor and

proliferator in prostate cancer. *Proc Natl Acad Sci U S A*. 2008;105(34):12182-12187. doi:10.1073/pnas.0804700105.

41. Parisotto M, Metzger D. Genetically engineered mouse models of prostate cancer. *Mol Oncol*. 2013;7(2):190-205. doi:10.1016/j.molonc.2013.02.005.

42. Kleeberger W, Bova GS, Nielsen ME, *et al.* Roles for the stem cell-associated intermediate filament nestin in prostate cancer migration and metastasis. *Cancer Res*. 2007;67(19):9199-9206. doi:10.1158/0008-5472.CAN-07-0806.

43. Xie Q, Liu Y, Cai T, Horton C, Stefanson J, Wang ZA. Dissecting cell-type-specific roles of androgen receptor in prostate homeostasis and regeneration through lineage tracing. *Nat Commun*. 2017;8:1-14. doi:10.1038/ncomms14284.

44. Niu Y, Chang T-M, Yeh S, Ma W-L, Wang YZ, Chang C. Differential androgen receptor signals in different cells explain why androgen-deprivation therapy of prostate cancer fails. *Oncogene*. 2010;29(25):3593-3604. doi:10.1038/onc.2010.121.

45. Mu P, Zhang Z, Benelli M, *et al.* SOX2 promotes lineage plasticity and antiandrogen resistance in TP53 - and RB1 -deficient prostate cancer. *Science (80-)*. 2017;355(6320):84-88. doi:10.1126/science.aah4307.

46. Patel LR, Camacho DF, Shiozawa Y, Pienta KJ, Taichman RS. Mechanisms of cancer cell metastasis to the bone: a multistep process. *Futur Oncol*. 2011;7(11):1285-1297. doi:10.2217/fon.11.112.

47. Ren G, Zhao X, Wang Y, *et al.* CCR2-dependent recruitment of macrophages by tumor-educated mesenchymal stromal cells promotes tumor development and is mimicked by TNFa. *Cell Stem Cell*. 2012;11(6):812-824. doi:10.1016/j.stem.2012.08.013.

48. Josson S, Matsuoka Y, Chung LWK, Zhau HE, Wang R. Tumor–stroma co-evolution in prostate cancer progression and metastasis. *Semin Cell Dev Biol*. 2010;21(1):26-32. doi:10.1016/j.semcdb.2009.11.016.

49. Hosaka K, Yang Y, Seki T, *et al.* Pericyte–fibroblast transition promotes tumor growth and metastasis. *Proc Natl Acad Sci*. 2016;113(38):E5618-E5627. doi:10.1073/pnas.1608384113.

50. Guise TA. Breast cancer bone metastases: It's all about the neighborhood. *Cell*. 2013;154(5):957-958. doi:10.1016/j.cell.2013.08.020.

51. Suetsugu A, Momiyama M, Hiroshima Y, *et al.* Color-Coded Imaging of Breast Cancer Metastatic Niche Formation in Nude Mice. *J Cell Biochem*. 2015;116(12):2730-2734. doi:10.1002/jcb.25227.

52. Kaplan RN, Riba RD, Zacharoulis S, et al. VEGFR1-positive haematopoietic bone marrow progenitors initiate the pre-metastatic niche. *Nature*. 2005;438(7069):820-827. doi:10.1038/nature04186.

53. Reagan MR, Rosen CJ. Navigating the bone marrow niche: translational insights and cancer-driven dysfunction. *Nat Rev Rheumatol*. 2015;12(3):154-168. doi:10.1038/nrrheum.2015.160.

54. Shiozawa Y, Pedersen E a., Havens AM, *et al.* Human prostate cancer metastases

target the hematopoietic stem cell niche to establish footholds in mouse bone marrow. *J Clin Invest*. 2011;121(4):1298–1312. doi:10.1172/JCI43414DS1.

55. Haider MT, Holen I, Dear TN, Hunter K, Brown HK. Modifying the osteoblastic niche with zoledronic acid in vivo-Potential implications for breast cancer bone metastasis. *Bone*. 2014;66:240-250. doi:10.1016/j.bone.2014.06.023.

56. Shiozawa Y, Berry JE, Eber MR, *et al.* The marrow niche controls the cancer stem cell phenotype of disseminated prostate cancer. *Oncotarget*. 2016;7(27):41217-41232. doi:10.18632/oncotarget.9251.

57. Cabarcas SM, Mathews LA, Farrar WL. The cancer stem cell niche-there goes the neighborhood? *Int J Cancer*. 2011;129(10):2315-2327. doi:10.1002/ijc.26312.

58. Houthuijzen JM, Daenen LGM, Roodhart JML, Voest EE. The role of mesenchymal stem cells in anti-cancer drug resistance and tumour progression. *Br J Cancer*. 2012;106(12):1901-1906. doi:10.1038/bjc.2012.201.

59. Roodhart JML, Daenen LGM, Stigter ECA, *et al.* Mesenchymal stem cells induce resistance to chemotherapy through the release of platinum-induced fatty acids. *Cancer Cell*. 2011;20(3):370-383. doi:10.1016/j.ccr.2011.08.010.

60. Brennen WN, Denmeade SR, Isaacs JT. Mesenchymal stem cells as a vector for the inflammatory prostate microenvironment. *Endocr Relat Cancer*. 2013;20(5):R269-290. doi:10.1530/ERC-13-0151.

61. Spaeth E, Klopp A, Dembinski J, Andreeff M, Marini F. Inflammation and tumor microenvironments: defining the migratory itinerary of mesenchymal stem cells. *Gene Ther*. 2008;15(10):730-738. doi:10.1038/gt.2008.39.

62. Wynn RF, Hart CA, Corradi-Perini C, *et al.* A small proportion of mesenchymal stem cells strongly expresses functionally active CXCR4 receptor capable of promoting migration to bone marrow. *Blood*. 2004;104(9):2643-2645. doi:10.1182/blood-2004-02-0526.

63. Corcoran KE, Trzaska KA, Fernandes H, *et al.* Mesenchymal stem cells in early entry of breast cancer into bone marrow. *PLoS One*. 2008;3(6):1-10. doi:10.1371/journal.pone.0002563.

64. Ip JE, Wu Y, Huang J, Zhang L, Pratt RE, Dzau VJ. Mesenchymal Stem Cells Use Integrin beta-1 Not CXC Chemokine Receptor 4 for Myocardial Migration and Engraftment. *Mol Biol Cell*. 2007;18(8):2873-282. doi:10.1091/mbc.E07.

65. Ye H, Cheng J, Tang Y, *et al.* Human bone marrow-derived mesenchymal stem cells produced TGFbeta contributes to progression and metastasis of prostate cancer. *Cancer Invest*. 2012;30(7):513-518. doi:10.3109/07357907.2012.692171.

66. Bergfeld SA, DeClerck YA. Bone marrow-derived mesenchymal stem cells and the tumor microenvironment. *Cancer Metastasis Rev*. 2010;29(2):249-261. doi:10.1007/s10555-010-9222-7.

67. McMillin DW, Delmore J, Weisberg E, *et al.* Tumor cell-specific bioluminescence platform to identify stroma-induced changes to anticancer drug activity. *Nat Med*. 2010;16(4):483-489. doi:10.1038/nm.2112.

68. Yu PF, Huang Y, Han YY, *et al.* TNFα-activated mesenchymal stromal cells promote breast cancer metastasis by recruiting CXCR2+ neutrophils. *Oncogene*. 2017;36(4):482-490. doi:10.1038/onc.2016.217.

69. Chowdhury R, Webber JP, Gurney M, Mason MD, Tabi Z, Clayton A. Cancer exosomes trigger mesenchymal stem cell differentiation into pro-angiogenic and pro-invasive myofibroblasts. *Oncotarget*. 2015;6(2):715-731. doi:10.18632/oncotarget.2711.

70. Liu S, Jiang M, Zhao Q, *et al.* Vascular endothelial growth factor plays a critical role in the formation of the pre-metastatic niche via prostaglandin E2. *Oncol Rep*. 2014;32(6):2477-2484. doi:10.3892/or.2014.3516.

71. Ridge SM, Sullivan FJ, Glynn SA. Mesenchymal stem cells: key players in cancer progression. *Mol Cancer*. 2017;16(1):31. doi:10.1186/s12943-017-0597-8.

72. Ono M, Kosaka N, Tominaga N, *et al.* Exosomes from bone marrow mesenchymal stem cells contain a microRNA that promotes dormancy in metastatic breast cancer cells. *Sci Signal*. 2014;7(332):1-10. doi:10.1126/scisignal.2005231.

73. Rhee HW, Zhau HE, Pathak S, *et al.* Permanent phenotypic and genotypic changes of prostate cancer cells cultured in a three-dimensional rotating-wall vessel. *Vitr Cell Dev Biol - Anim*. 2001;37(3):127. doi:10.1290/1071-2690(2001)037<0127:PPAGCO>2.0.CO;2.

74. Luo J, Ok Lee S, Liang L, *et al.* Infiltrating bone marrow mesenchymal stem cells increase prostate cancer stem cell population and metastatic ability via secreting cytokines to suppress androgen receptor signaling. *Oncogene*. 2014;33(21):2768-2778. doi:10.1038/onc.2013.233.

75. Cheng J, Yang K, Zhang Q, *et al.* The role of mesenchymal stem cells in promoting the transformation of androgen-dependent human prostate cancer cells into androgen-independent manner. *Sci Rep*. 2016;6(1):16993. doi:10.1038/srep16993.

76. Fuzio P, Ditonno P, Rutigliano M, *et al.* Regulation of TGF-β1 expression by Androgen Deprivation Therapy of prostate cancer. *Cancer Lett*. 2012;318(2):135-144. doi:10.1016/j.canlet.2011.08.034.

77. Yano S, Miwa S, Mii S, *et al.* Invading cancer cells are predominantly in G0/G1 resulting in chemoresistance demonstrated by real-time FUCCI imaging. *Cell Cycle*. 2014;13(6):953-960. doi:10.4161/cc.27818.

78. Bhola NE, Balko JM, Duggar TC, *et al.* TGF-β Inhibition enhances chemotherapy action against triple-negative breast cancer. *J Clin Investig*. 2013;123(3):1348-1358. doi:10.1172/JCI65416DS1.

79. Placencio VR, Sharif-Afshar AR, Li X, *et al.* Stromal transforming growth factor-β signaling mediates prostatic response to androgen ablation by paracrine Wnt activity. *Cancer Res*. 2008;68(12):4709-4718. doi:10.1158/0008-5472.CAN-07-6289.

80. Sramkoski RM, Pretlow TG, Giaconia JM, *et al.* A new human prostate carcinoma cell line, 22Rv1. *In Vitro Cell Dev Biol Anim*. 1999;35(7):403-409. doi:10.1007/s11626-999-0115-4.

81. Wikström P, Stattin P, Franck-Lissbrant I, Damber JE, Bergh A. Transforming growth

factor beta1 is associated with angiogenesis, metastasis, and poor clinical outcome in prostate cancer. *Prostate*. 1998;37(1):19-29. http://www.ncbi.nlm.nih.gov/pubmed/9721065.

82. Placencio VR, Li X, Sherrill TP, Fritz G, Bhowmick NA. Bone marrow derived mesenchymal stem cells incorporate into the prostate during regrowth. *PLoS One*. 2010;5(9):1-9. doi:10.1371/journal.pone.0012920.

83. Hall CL, Kang S, MacDougald OA, Keller ET. Role of Wnts in prostate cancer bone metastases. *J Cell Biochem*. 2006;97(4):661-672. doi:10.1002/jcb.20735.

84. Wainstein MA, He F, Robinson D, *et al.* CWR22: androgen-dependent xenograft model derived from a primary human prostatic carcinoma. *Cancer Res*. 1994;54(23):6049-6052.

85. Nagabhushan M, Miller CM, Pretlow TP, *et al.* CWR22: The first human prostate cancer xenograft with strongly: Androgen-dependent and relapsed strains both in vivo and in soft agar. *Cancer Res*. 1996;56(13):3042-3046.

86. Watson PA, Ellwood-Yen K, King JC, Wongvipat J, LeBeau MM, Sawyers CL. Context-dependent hormone-refractory progression revealed through characterization of a novel murine prostate cancer cell line. *Cancer Res*. 2005;65(24):11565-11571. doi:10.1158/0008-5472.CAN-05-3441.

87. Reznikoff C, Brankow DW, Heidelberger C. Establishment and Characterization of a Cloned Line of C3H Mouse Embryo Cells Sensitive to Postconfluence Inhibition of Division Establishment and Characterization of a Cloned Line of C3H Mouse Embryo Cells Sensitive to Postconfluence Inhibition of. *Cancer Res*. 1973;33(12):3231-3238.

88. Djouad F, Plence P, Bony C, *et al.* Immunosuppressive effect of mesenchymal stem cells favors tumor growth in allogeneic animals. *Blood*. 2003;102(10):3837-3844. doi:10.1182/blood-2003-04-1193.

89. Chamberlain G, Wright K, Rot A, Ashton B, Middleton J. Murine mesenchymal stem cells exhibit a restricted repertoire of functional chemokine receptors: Comparison with human. *PLoS One*. 2008;3(8):1-6. doi:10.1371/journal.pone.0002934.

90. Zhao L, Li G, Chan KM, Wang Y, Tang PF. Comparison of multipotent differentiation potentials of murine primary bone marrow stromal cells and mesenchymal stem cell line C3H10T1/2. *Calcif Tissue Int*. 2009;84(1):56-64. doi:10.1007/s00223-008-9189-3.

91. Mosmann T. Rapid colorimetric assay for cellular growth and survival: Application to proliferation and cytotoxicity assays. *J Immunol Methods*. 1983;65(1-2):55-63. doi:10.1016/0022-1759(83)90303-4.

92. van de Loosdrecht AA, Beelen RHJ, Ossenkoppele GJ, Broekhoven MG, Langenhuijsen MMAC. A tetrazolium-based colorimetric MTT assay to quantitate human monocyte mediated cytotoxicity against leukemic cells from cell lines and patients with acute myeloid leukemia. *J Immunol Methods*. 1994;174(94):311-320. doi:10.1016/0022-1759(94)90034-5.

93. O'Brien J, Wilson I, Orton T, Pognan F. Investigation of the Alamar Blue (resazurin) fluorescent dye for the assessment of mammalian cell cytotoxicity. *Eur J Biochem*. 2000;267(17):5421-5426. doi:10.1046/j.1432-1327.2000.01606.x.

94. Zhang, Chung, Oldenburg. A Simple Statistical Parameter for Use in Evaluation and Validation of High Throughput Screening Assays. *J Biomol Screen*. 1999;4(2):67-73. doi:10.1177/108705719900400206.

95. Iversen PW, Beck B, Chen Y-F, *et al.* HTS Assay Validation. In: Sittampalam G, Coussens N, Brimacombe K, eds. *Assay Guidance Manual [Internet]*. Bethesda (MD): Eli Lilly & Company and the National Center for Advancing Translational Sciences; 2012. http://www.ncbi.nlm.nih.gov/pubmed/22553862.

96. Macarron R, Banks MN, Bojanic D, *et al.* Impact of high-throughput screening. *Nature*. 2011;10(March 2011):188-195. doi:10.1038/nrd3368.

97. Hertzberg RP, Pope AJ. High-throughput screening: New technology for the 21st century. *Curr Opin Chem Biol*. 2000;4(4):445-451. doi:10.1016/S1367-5931(00)00110-1.

98. Isherwood BJ, Walls RE, Roberts ME, *et al.* High-Content Analysis to Leverage a Robust Phenotypic Profiling Approach to Vascular Modulation. *J Biomol Screen*. 2013;18(10):1246-1259. doi:10.1177/1087057113499775.

99. Warchal SJ, Dawson JC, Carragher NO. Development of the Theta Comparative Cell Scoring Method to Quantify Diverse Phenotypic Responses Between Distinct Cell Types. *Assay Drug Dev Technol*. 2016;14(7):395-406. doi:10.1089/adt.2016.730.

100. Uphoff CC, Drexler HG. in Cell Cultures by Polymerase Chain Reaction. In: Langdon SP, ed. *Methods in Molecular Medicine: Cancer Cell Culture: Methods and Protocols*. Vol 88. 1st ed. Totowa, NJ: Humana Press Inc.; 2004:319-326.

101. Skardal A, Devarasetty M, Rodman C, Atala A, Soker S. Liver-Tumor Hybrid Organoids for Modeling Tumor Growth and Drug Response In Vitro. *Ann Biomed Eng*. 2015;43(10):2361-2373. doi:10.1007/s10439-015-1298-3.

102. Shackleton M, Quintana E, Fearon ER, Morrison SJ. Heterogeneity in Cancer: Cancer Stem Cells versus Clonal Evolution. *Cell*. 2009;138(5):822-829. doi:10.1016/j.cell.2009.08.017.

103. Cao Z, West C, Norton-Wenzel CS, *et al.* Effects of resin or charcoal treatment on fetal bovine serum and bovine calf serum. *Endocr Res*. 2009;34(4):101-108. doi:10.3109/07435800903204082.

104. Faber PW, King A, van Rooij HC, Brinkmann AO, de Both NJ, Trapman J. The mouse androgen receptor. Functional analysis of the protein and characterization of the gene. *Biochem J*. 1991;278:269-278.

105. Hamid R, Rotshteyn Y, Rabadi L, Parikh R, Bullock P. Comparison of alamar blue and MTT assays for high through-put screening. *Toxicol Vitr*. 2004;18(5):703-710. doi:10.1016/j.tiv.2004.03.012.

106. Plumb J a, Milroy R, Kaye SB. Effects of the pH Dependence of 3- (4 , 5-Dimethylthiazol-2-yl) -2 , 5-diphenyl- tetrazolium Bromide-Formazan Absorption on Chemosensitivity Determined by a Novel Tetrazolium-based Assay1. *Cancer Res*. 1989;49:4435-4440.

107. Wang L, Sun J, Horvat M, Koutalistras N, Johnston B, Ross Sheil A. Evaluation of MTS, XTT, MTT and3HTdR incorporation for assessing hepatocyte density, viability and

proliferation. *Methods Cell Sci*. 1996;18(3):249-255. doi:10.1007/BF00132890.

108. Petty R, Sutherland L, Hunter E, Cree I. Comparison of MTT and ATP-based assays for the measurement of viable cell number. *J Biolumin Chemilumin*. 1995;10(1):29-34.

109. Rajwa B. Effect-Size Measures as Descriptors of Assay Quality in High-Content Screening: A Brief Review of Some Available Methodologies. *Assay Drug Dev Technol*. 2017;15(1):15-29. doi:10.1089/adt.2016.740.

110. Meijer TG, Jager A, Gent DC Van. Ex vivo tumor culture systems for functional drug testing and therapy response prediction. *Futur Sci OA*. 2017;3(2):FSO190. doi:10.4155/fsoa-2017-0003.

111. Boehnke K, Iversen PW, Schumacher D, *et al.* Assay Establishment and Validation of a High-Throughput Screening Platform for Three-Dimensional Patient-Derived Colon Cancer Organoid Cultures. *J Biomol Screen*. 2016;21(9):931-941. doi:10.1177/1087057116650965.

112. Beachley VZ, Wolf MT, Sadtler K, *et al.* Tissue matrix arrays for high throughput screening and systems analysis of cell function. *Nat Methods*. 2015;12(12):1197-1204. doi:10.1038/nmeth.3619.Tissue.